Dissertation

Biotransformations from and to methylated flavonoids

Subtitle

Benjamin Weigel
Leibniz-Institute of Plant Biochemistry
Department of Bioorganic Chemistry
Weinberg 3
06120 Halle(Saale)
June 12, 2015

Advisor: Prof. Dr. Ludger A. Wessjohann
wessjohann@ipb-halle.de
+49 (345) 5582-1301

noch nicht bekannt

Contents

List of Figures

List of Tables

Notes of Revisors

Preface

1 Abstracts

1.1 English Abstract

Test Lorem ipsum dolor sit amet, consectetuer adipiscing elit. Ut purus elit, vestibulum ut, placerat ac, adipiscing vitae, felis. Curabitur dictum gravida mauris. Nam arcu libero, nonummy eget, consectetuer id, vulputate a, magna. Donec vehicula augue eu neque. Pellentesque habitant morbi tristique senectus et netus et malesuada fames ac turpis egestas. Mauris ut leo. Cras viverra metus rhoncus sem. Nulla et lectus vestibulum urna fringilla ultrices. Phasellus eu tellus sit amet tortor gravida placerat. Integer sapien est, iaculis in, pretium quis, viverra ac, nunc. Praesent eget sem vel leo ultrices bibendum. Aenean faucibus. Morbi dolor nulla, malesuada eu, pulvinar at, mollis ac, nulla. Curabitur auctor semper nulla. Donec varius orci eget risus. Duis nibh mi, congue eu, accumsan eleifend, sagittis quis, diam. Duis eget orci sit amet orci dignissim rutrum.

1.2 Deutsche Zusammenfassung

Nam dui ligula, fringilla a, euismod sodales, sollicitudin vel, wisi. Morbi auctor lorem non justo. Nam lacus libero, pretium at, lobortis vitae, ultricies et, tellus. Donec aliquet, tortor sed accumsan bibendum, erat ligula aliquet magna, vitae ornare odio metus a mi. Morbi ac orci et nisl hendrerit mollis. Suspendisse ut massa. Cras nec ante. Pellentesque a nulla. Cum sociis natoque penatibus et magnis dis parturient montes, nascetur ridiculus mus. Aliquam tincidunt urna. Nulla ullamcorper vestibulum turpis. Pellentesque cursus luctus mauris.

II

Thesis

2 Introduction

Some introductionary text

2.1 Natural products and secondary metabolites

2.1.1 General

2.1.2 Classes of natural products

Terpenoids and Steroids

... here is some text

Polyketides and non-ribosomal peptides

... here is some text

Alkaloids

... here is some text

Phenylpropanoids

... here is some text Flavonoids and phenyl propanoids have important functions in nature and can function as protection against high UV-exposure, signaling molecules or transcriptional regulators [35, 5].

2.2 Alkylating reactions in nature

2.2.1 Methylation

2.2.2 Prenylation

2.2.3 Glycosylation

2.3 Usage and expansion of natures reaction toolbox

2.3.1 Terpene synthases and elongases

2.3.2 Methyl transferases

2.3.3 Glycosyl transferases

2.3.4 Other important enzymes in biotech research

BMVOs

Esterases/Lipases

Oxidases

Lyases

Transaminases

2.4 Conclusion

c

3 Material And Methods

Within this section percentages refer to volume per volume (v/v) percentages unless otherwise specified.

3.1 Materials

3.1.1 Chemicals

Enzymes and buffers used for molecular cloning were obtained from Life Technologies (Darmstadt, Germany), unless otherwise noted. Flavonoid HPLC standards were purchased from Extrasynthese (Genay, France). Deuterated solvents were aquired from Deutero GmbH (Kastellaun, Germany). Solvents, purchased from VWR (Poole, England), were distilled in-house before use.
All other chemicals were obtained from either Sigma-Aldrich (Steinheim, Germany), Applichem (Darmstadt, Germany), Carl Roth (Karlsruhe, Germany) or Merck (Darmstadt, Germany).

3.1.2 Commonly used solutions and buffers

50× 5052	25 % glycerol, 2.5 % (w/v) glucose, 10 % (w/v) α-lactose
binding buffer	50 mM Tris/HCl, 500 mM NaCl, 10 % glycerol, 2.5 mM imidazole pH 7
elution buffer	50 mM Tris/HCl, 500 mM NaCl, 10 % glycerol, 250 mM imidazole pH 7
lysis buffer	50 mM Tris/HCl, 500 mM NaCl, 10 % glycerol, 2.5 mM imidazole, 0.2 % Tween-20 pH 7
1 M MMT pH 4 (10×)	26.8 g/l L-malic acid, 78.1 g/l MES, 26.8 g/l Tris, 2.1 % 10 M HCl
1 M MMT pH 9 (10×)	26.8 g/l L-malic acid, 78.1 g/l MES, 26.8 g/l Tris, 6.7 % 10 M NaOH
20× NPS	1 M Na_2HPO_4, 1 M KH_2PO_4, 0.5 M $(NH_4)_2SO_4$

1 M SSG pH 4 (10×)	14.8 g/l succinic acid, 60.4 g/l $NaH_2PO_4 \cdot H_2O$, 32.8 g/l glycine, 0.4 % 10 M NaOH
1 M SSG pH 10 (10×)	14.8 g/l succinic acid, 60.4 g/l $NaH_2PO_4 \cdot H_2O$, 32.8 g/l glycine, 10.3 % 10 M NaOH
5× SDS sample buffer	10 % (w/v) SDS, 10 mM β-mercaptoethanol, 20 % glycerol, 0.2 M Tris/HCl pH 6.8, 0.05 % (w/v) bromophenolblue
1000× trace elements	50 mM $FeCl_3$, 20 mM $CaCl_2$, 10 mM $MnCl_2$, 10 mM $ZnSO_4$, 2 mM $CoCl_2$, 2 mM $CuCl_2$, 2 mM $NiCl_2$, 2 mM Na_2MoO_4, 2 mM Na_2SeO_3, 2 mM H_3BO_3

Preparation of natural deep eutectic solvent (NADES)

NADES were prepared by adding each component in a round-bottom flask with a stirrer and stirring the mixture at 50 °C with intermittent sonication treatments until a clear solution was obtained.

Table 3.1.: NADES-mixtures used within this work.

name	composition	mole ratio	mass fraction (w/w)
PCH	propane-1,2-diol	1:1:1	0.326
	choline chloride		0.597
	water		0.077
GCH	L-glucose	2:5:5	0.314
	choline chloride		0.608
	water		0.078

3.1.3 Culture media used to grow bacteria

LB-medium	10 g/l NaCl, 10 g/l tryptone, 5 g/l yeast extract, pH 7.5
LB-agar	LB + 1.5 % (w/v) agar-agar
TB-medium	12 g/l tryptone, 24 g/l yeaxst extract, 0.4 % glycerol, 72 mM K_2HPO_4, 17 mM KH_2PO_4
ZY	10 g/l tryptone, 5 g/l yeast extract
ZYP-5052	volume fraction (v/v): 0.928 ZY, 0.05 20× NPS, 0.02 50× 5052, 0.002 1 M $MgSO_4$, 0.0002 1000× trace elements

3.1.4 Bacterial strains

E.coli

BL21(DE3)	F$^-$ *ompT hsdSB*(r_B^-,m_B^-) *gal dcm* λ(DE3) Invitrogen, Karslruhe (Germany)
C41(DE3)	F$^-$ *ompT hsdSB*(r_B^-,m_B^-) *gal dcm* λ(DE3) Lucigen, Wisconsin (USA)
C43(DE3)	F$^-$ *ompT hsdSB*(r_B^-,m_B^-) *gal dcm* λ(DE3) Lucigen, Wisconsin (USA)
DH5α	F$^-$ Φ80*lacZ*ΔM15 Δ(*lacZYA-argF*) U169 *recA*1 *endA*1 *hsdR*17($r_K^-m_K^+$) *phoA supE*44 λ^- *thi*-1 *gyrA*96 *relA*1 Invitrogen, Karslruhe (Germany)
JM110	*rpsL thr leu thi lacY galK galT ara tonA tsx dam dcm glnV*44 Δ(*lac-proAB*) e14- [F' *traD*36 *proAB*$^+$ *lacI*^{q} *lacZ*ΔM15] *hsdR*17($r_K^-m_K^+$) Martin-Luther-University Halle-Wittenberg
JW1593 (BW25113 derivative)	*rrnB* Δ*lacZ*4787 *HsdR*514 Δ(*araBAD*)568 *rph*-1 Δ*ydgG* (Kan^R) Keio Collection, National Institute of Genetics (Japan)
MG1655	F$^-$ λ^- *ilvG*$^-$ *rfb*-50 *rph*-1 DSMZ, Hamburg (Germany)
One Shot TOP10	F$^-$ Φ80*lacZ*ΔM15 Δ(*mrr-hsdRMS-mcrBC*) *recA*1 *endA*1 *mcrA* Δ*lacX*74 *araD*139 Δ(*ara-leu*)7697 *galU galK rpsL* (Str^R) λ^- *nupG* Invitrogen, Karslruhe (Germany)
Origami(DE3)	Δ(*ara-leu*)7697 Δ*lacX*74 Δ*phoA Pvull phoR araD*139 *ahpC galE galK rpsL* F'[*lac + lacI q pro*] (DE3)*gor*522::*Tn*10 *trxB* (Kan^R, Str^R, Tet^R) Novagen, Wisconsin (USA)
Rosetta(DE3)	F$^-$ *ompT hsdSB*(r_B^-,m_B^-) *gal dcm* λ(DE3) pRARE (Cam^R) Novagen, Wisconsin (USA)
Rosetta(DE3) pLysS	F$^-$ *ompT hsdSB*(r_B^-,m_B^-) *gal dcm* λ(DE3) pLysSRARE (Cam^R) Novagen, Wisconsin (USA)
T7 Express	*fhuA*2 *lacZ::T7 gene*1 *[lon] ompT gal sulA*11 *R*(*mcr-*73::*miniTn*10–Tet^S)2 *[dcm] R*(*zgb-*210::*Tn*10–Tet^S) *endA*1 Δ(*mcrC-mrr*)114::*IS*10 NEB, Massachusetts (USA)

Agrobacterium tumefaciens

GV3101	chromosomal background: C58, marker gene: *rif*, Ti-plasmid: cured, opine: nopaline Sylvestre Marillonet, IPB

3.1.5 Plasmids

Table 3.3.: Plasmids used in this work.

name	supplier/source
pACYCDuet-1	Merck, Darmstadt (Germany)
pCDFDuet-1	Merck, Darmstadt (Germany)
pET-20b(+)	Merck, Darmstadt (Germany)
pET-28a(+)	Merck, Darmstadt (Germany)
pET-32a(+)	Merck, Darmstadt (Germany)
pET-41a(+)	Merck, Darmstadt (Germany)
pQE30	QIAGEN, Hilden (Germany)
pUC19	Invitrogen, Karslruhe (Germany)

3.1.6 Oligonucleotides and synthetic genes

Oligonucleotides and primers were ordered from Eurofins Genomics (Ebersberg, Germany). The purity grade was *high purity salt free* (HPSF). Synthetic genes or gene fragments were obtained from GeneArt® (Life Technologies, Darmstadt, Germany) or Eurofins Genomics (Ebersberg, Germany).

BWEIGEL: needs completion

Table 3.4.: Primers used in this work. Recognition sites for endonucleases are underlined. Positions used for site directed mutagenesis are in lower case font.

name	sequence (5'→3')	cloning site
somt1	TTG AAG ACA AAA TGG CTT CTT CAT TAA ACA ATG GCC G	BpiI
somt2	TTG AAG ACA AGG ACA CCC CAA ATA CTG TGA GAT CTT CC	BpiI
somt3	TTG AAG ACA AGT CCT TAG GAA CAC CTT TCT GGG AC	BpiI
somt4	TTG AAG ACA AAA GCT CAA GGA TAG ATC TCA ATA AGA GAC	BpiI
pfomt1.fw	CAG AGA GGC cTA TGA GAT TGG CTT GC	
pfomt1.rv	GCA AGC CAA TCT CAT AgG CCT CTC TG	
pfomt2.fw	CAT ATG GAT TTT GCT GTG ATG AAG CAG GTC	NdeI
pfomt2.rv	GAA TTC AAT AAA GAC GCC TGC AGA AAG TG	EcoRI
pRha1.fw	CTC TAG CAG ATC TCG GTG AGC ATC ACA TCA CCA CAA TTC	BglII
pRha1.rv	CAA TTG AGG ATC CCC ATT TTA ACC TCC TTA GTG	BamHI
pUC1.fw	GCG TAT TGG Gag aTC TTC CGC TTC CTC	
pUC1.rv	GAG GAA GCG GAA GAt ctC CCA ATA CGC	

3.1.7 Instruments

CD-spectrometer	Jasco J-815 (Eaton, USA)
electrophoresis (horizontal)	Biometra Compact XS/S (Göttingen, Germany)
electrophoresis (vertical)	Biometra Compact M (Göttingen, Germany) Biometra Minigel-Twin (Göttingen, Germany)
FPLC	ÄKTA purifier (GE Healthcare, Freiburg, Germany)
GC/MS	GC-MS-QP2010 Ultra (Shimadzu, Duisburg, Germany)
HPLC	VWR-Hitachi LaChrom Elite (VWR, Darmstadt, Germany)
ITC	MicroCal iTC200 (Malvern, Worcestershire, UK)
plate-reader	SpectraMax M5 (Molecular Devices, Biberach, Germany)
NMR-spectrometer	Varian Unity 400 (Agilent, Böblingen, Germany) Varian VNMRS 600 (Agilent, Böblingen, Germany)
photospectrometer	Eppendorf Biophotometer Plus (Hamburg, Germany) JASCO V-560 (Eaton, USA) Colibri Microvolume Spectrometer (Biozym, Hess. Oldendorf, Germany)
centrifuges	Eppendorf 5424 (Hamburg, Germany) Hettich Mikro 120 (Kirchlengern, Germany) Beckman Avanti J-E, Beckman Allegra X-30R (Krefeld, Germany)
centrifuge rotors	Beckman JA-10, JA-16.250, JS-4.3 (Krefeld, Germany)

3.1.8 Software

All mathematical and statistical computations and graphics were done with the R software (versions 3.1.X, *http://cran.r-project.org/*) [83]. Visualizations of macromolecules were arranged using the PyMol Molecular Graphics System, version 1.7.0.0 (Schrödinger, New York, USA).
Physicochemical calculations and calculations of different molecular descriptors were performed using Marvin Beans 15.4.13.0 (ChemAxon, Budapest, Hungary) and Molecular Operating Environment 2008.10 (Chemical Computing Group, Montreal, Canada). Special software used for X-ray crystal structure solution is discussed seperately in the corresponding section (3.5).

3.2 Molecular Biology

Basic molecular biology methods like polymerase chain reaction (PCR), DNA restriction/ligation, DNA gel electrophoresis, preparation of competent cells and

transformation were performed based on the protocols summarized by Sambrook and Russell [91].
Plasmid DNA was isolated using the QIAprep® Spin Miniprep Kit (QIAGEN, Hilden, Germany) according to the manufacturer's instructions.
In vitro site-directed mutatgenesis was set-up according to the protocol of the *QuikChange™ Site-Directed Mutagenesis* kit [2] offered by Agilent Technologies (Santa Clara, USA).
Nucleotide fragments obtained by PCR, restriction/ligation procedures or excision from electrophoresis gels were purified and concentrated using the *Nucleospin Gel and PCR Clean-up* kit provided by Machery-Nagel (Düren, Germany) according to the instructions provided by the manufacturer.

3.2.1 Golden Gate Cloning

The Golden Gate cloning procedure is a one-pot method, meaning the restriction digestion and ligation are carried out in the same reaction vessel at the same time [51, 26]. Consequently PCR-fragments, destination vector, restriction endonuclease and ligase are added together in this reaction. The methodology employs type II restriction enzymes, which together with proper design of the fragments allow for a ligation product lacking the original restriction sites.
For digestion/ligation reactions of fragments containing BpiI sites, 20 fmol of each fragment or vector, together with 5 U of BpiI and 5 U of T4 ligase were combined in a total volume of 15 µl 1× ligase buffer. For fragments to be cloned via BsaI sites, BpiI in the above reaction was substituted by 5 U BsaI.
The reaction mixture was placed in a thermocycler and inbcubated at 37 °C for 2 min and 16 °C for 5 min. These two first steps were repeated 50 times over. Finally, the temperature was raised to 50 °C (5 min) and 80 °C (10 min) to inactivate the enzymes.

3.2.2 Subcloning of genes

All subcloning procedures were performed according to section 3.2 and specifically subsection 3.2.1. Specific steps for the subcloning of any genes discussed can be found in the appendix (p.48). The *pfomt* gene was subcloned from the pQE-30 vector kindly provided by Thomas Vogt (Leibniz-Institute of Plant Biochemistry (IPB), Halle, Germany) into the pET-28a(+) vector. The *somt-2* gene was subcloned from the pQE-30 vector kindly provided by Martin Dippe (IPB, Halle, Germany) into the pET-28-MC vector.

3.2.3 Transformation of electrocompetent *Agrobacterium tumefaciens* cells

A 50 µl aliquot of electrocompetent *A. tumefaciens* cells was thawed on ice. (50 to 100) ng of plasmid were added, the solution was mixed gently and transferred to a pre-cooled electroporation cuvette. After pulsing (2.5 kV, 200 Ω) 1 ml of lysogeny broth (LB)-medium was added, the mixture transferred to a 1.5 ml tube and incubated for (3 to 4) hours at 28 °C. The culture was centrifuged (10 000 × *g*, 1 min) and 900 µl supernatant were discarded. The pellet was resuspended in the remaining liquid, plated onto LB-agar plates supplemented with 40 µg/ml rifampicin and 50 µg/ml carbencillin and incubated at 28 °C for (2 to 3) days.

3.3 Treatment of plant material

3.3.1 Infiltration of *Nicotiana benthamiana*

Before infiltration *N. benthamiana* plants were pruned, such that only leaves to be infiltrated remained with the plant. 5 ml cultures of transformed *A. tumefaciens* in LB-medium (with 40 µg/ml rifampicin and 50 µg/ml carbencillin) were grown over night at 28 °C and 220 rpm. OD^{600} of the culture was measured and adjusted to 0.2 by dilution with infiltration buffer (10 mM MES/NaOH, 10 mM $MgSO_4$ pH 5.5). When multiple *A. tumefaciens* transformed with different contructs/plasmids were used for infiltration, the cultures were mixed and diluted using infiltration buffer, such that OD^{600} of each culture in the mix was 0.2. The solution was infiltrated into the abaxial side of *N. benthamiana* leaves using a plastic syringe. The leaf material was harvested after 7 days.

3.3.2 Plant material harvest

Infiltrated/Infected areas of *N. benthamiana* leaf material were cut out and grouped by plant number, leaf position (top/bottom) and leaf side (right/left). The grouped clippings were weighed, frozen in liquid nitrogen, ground to a powder, freeze-dried and stored at −80 °C.

3.3.3 Extraction of flavonoids from *N. benthamiana* leaves

Two tips of a small spatula of freeze-dried material (≈6 mg), were weighed exactly and extracted with 500 µl 75 % aqueous methanol containing 1 mM ascorbic acid, 0.2 % formic acid and 0.1 mM flavone (internal standard). Therefore the suspension was vortexed for 30 s, rotated on an orbital shaker for 10 min and vortexed again for

30 s. The suspension was centrifuged (20 000 × g, 4 °C, 10 min) and the supernatant transferrerd to a new tube, to remove the insoluble plant material. The supernatant was centrifuged again (20 000 × g, 4 °C, 10 min) and the resulting supernatant was transferred to a HPLC-vial and stored at −20 °C until analysis.

3.4 Protein biochemistry

Stock solutions of antibiotics, IPTG or sugars were prepared according to the pET System Manual by Novagen [78], unless otherwise noted.

3.4.1 Determination of protein concentration

Protein concentrations were estimated using the absorption of protein solutions at 280 nm, which is mainly dependent on the amino acid composition of the protein studied [33]. Extinction coefficients of proteins were calculated from the amino acid sequence using the ExpPASy servers's ProtParam tool [32].

Table 3.6.: *Calculated extinction coefficients of proteins used in this work.*

protein/enzyme	$\varepsilon_{280\text{nm}}^{1\text{ g/l}}$ in ml mg^{-1} cm^{-1}
PFOMT (reduced)	0.714
PFOMT Y51K N202W (reduced)	0.852
SOMT-2 (oxidized)	1.263
SOMT-2 (reduced)	1.247
COMT	

3.4.2 Protein production test (expression test)

The heterologous production of proteins in *E. coli* was assessed in a small scale protein production test, henceforth called expression test. Single colonies of *E. coli* transformed with the constructs to be studied were used to inoculate a 2 ml starter culture in LB-medium containing the appropriate antibiotics. The working concentrations of antiobiotics used was as follows: 200 µg/ml ampicillin, 150 µg/ml kanamycin, 50 µg/ml chloramphenicol, 20 µg/ml tetracycline.
The starter culture was allowed to grow at 37 °C and 200 rpm over night. A 5 ml sampling culture of the medium to be studied containing the appropriate antibiotics was prepared. The media tested included LB, terrific broth (TB) and auto-induction media like ZYP-5052. The sampling culture was inoculated to an OD^{600} of 0.075 using the starter culture and incubated at different temperatures and 200 rpm in a

shaking incubator. 1 mM isopropyl-D-thiogalactopyranosid (IPTG) was added when the OD^{600} reached 0.6-0.8, if appropriate for the studied construct. 1 ml samples were removed after different times of incubation (e.g. 4, 8, 12 hours), subfractionated (3.4.3) and analyzed via SDS-polyacrylamide gel electrophoresis (PAGE) (3.4.6). Exact specifications of growth conditions (e.g. temperature, time, constructs) are discussed in the individual sections.

3.4.3 Protein subfractionation

The protein subfractionation procedure described herein was adapted from the protocol described in the pET Manual [78]. Overall 5 protein subfractions can be obtained, including *total cell protein, culture supernatant (medium) protein, periplasmic protein, solube cytoplasmic protein* and *insoluble protein.*
The OD^{600} of the culture sample was measured and the cells harvested by centrifugation at 10 000 × *g*, 4 °C for 5 minutes. The protein in the supernatant medium was concentrated by precipitation with trichloro acetic acid (TCA) (3.4.4) for SDS-PAGE analysis. The periplasmic protein was prepared (3.4.5) and also concentrated by TCA precipitation for SDS-PAGE. Cells were lysed by resuspending the cell pellet in (OD^{600} × V × 50) µl of bacterial protein extraction reagent (B-PER) and vortexing vigorously for 30 s. The suspension was incubated at room temperature (RT) for 30 min to assure complete lysis. To separate insoluble protein and cell debris from the soluble cytosolic protein, the suspension was centrifuged at 10 000 × *g* and 4 °C for 10 min. Soluble cytoplasmic protein was contained in the supernatant, whereas insoluble protein remained in the pellet. For SDS-PAGE analysis of the insoluble protein, the pellet was resuspended in the same volume of B-PER. To obtain only the total cell protein fraction, the preparation of periplasmic and soluble cytosolic protein was omitted. Sample volumes of 10 µl of each fraction were used for SDS-PAGE analysis.

3.4.4 Protein sample concentration by TCA precipitation

Diluted protein samples were concetrated by TCA precipitation in microcentrifuge tubes. Therefore 0.1 volume (V) of 100 % (w/v) TCA in water was added to the clarified sample, which was then vortexed for 15 s and placed on ice for a minimum of 15 min. The sample was centrifuged at 14 000 × *g*, 4 °C for 15 min. The supernatant was discarded and the pellet was washed twice with 0.2 V ice-cold acetone. The acetone was removed and the pellet set to air-dry in an open tube. After drying, the protein pellet was resuspended in 0.1 V phosphate buffered saline (PBS) containing 1 × SDS-sample buffer by heating to 85 °C and vigorous vortexing, to achieve a

10 × concentration. After resuspension the sample was analyzed by SDS-PAGE or stored at −20 °C until use.

3.4.5 Preparation of periplasmic protein

Target proteins may be directed to the periplasmic space by N-terminal signal sequences like *pelB* or *DsbA/C* [66]. The periplasma is, other than the cytosol, an oxidizing environment and often used for the production of proteins containing dilsufide linkages. The preparation of periplasmic protein was accomplished by an osmotic shock protocol modified from Current Protocols in Molecular Biology [7]. The cell pellet was resuspended in the same volume as the culture sample of 30 mM tris-HCl, 20 % (w/v) sucrose, pH 8 and 1 mM ethylenediaminetetraacetic acid (EDTA) was added. The suspension was stirred for 10 min at RT and the cells were collected by centrifugation at 10 000 × g, 4 °C for 10 min. The supernatant was discarded and the cell pellet was resuspended in the same volume of ice-cold 5 mM $MgSO_4$. The suspension was stirred for 10 min on ice, while the periplasmic proteins were released into the solution. The cells were collected by centrifugation as before. Periplasmic proteins were contained in the supernatant.

3.4.6 Discontinous SDS-polyacrylamide gel electrophoresis (SDS-PAGE)

The analysis of samples via SDS-PAGE was realized via the discontinous system first described by Laemmli, which allows separation of proteins based on their electrophoretic mobility, which in turn depends on their size [54].
The SDS-PAGE procedure was carried out according to standard protocols described by Sambrook and Russell [91]. Very dilute and/or samples with high ionic strength were concentrated and/or desalted by the TCA precipitation procedure described in subsection 3.4.4. Generally a 10 % (acrylamide/bisacrylamide) running gel combined with a 4 % stacking gel was used. Reducing SDS-PAGE sample buffer was added to the protein sample to be analyzed, whereafter the sample was heated to 95 °C for 5 min, to allow for total unfolding of the protein. After cooling to RT the samples were transferred into the gel pockets for analysis. The *PageRuler™ Prestained Protein Ladder* (Life Technologies GmbH, Darmstadt, Germany) was used as a molecular weight (MW) marker and run alongside every analysis as a reference. Gels were stained using a staining solution of 0.25 % Coomassie Brilliant Blue G-250 (w/v) in water:methanol:acetic acid (4:5:1) and destained by treatment with water:methanol:acetic acid (6:3:1).

3.4.7 Buffer change of protein samples

The buffer in protein samples was exchanged either by dialysis, or by centrifugal filter concentrators (Amicon® Ultra Centrifugal Filter; Merck, Darmstadt, Germany). Large volumes of highly concentrated protein solutions were preferably dialyzed. Respectively, very dilute samples were concentrated and rebuffered using centrifugal concentrators.

Dialysis was carried out at least twice against a minimum of 100 times the sample volume. Dialysis steps were carried out at RT for 2 hours, or over-night at 4 °C. Centrifugal concentrators were used according to the manufacturers instructions.

3.4.8 Production of recombinant protein

Heterologous production of PFOMT

PFOMT was produced as a N-terminally $(His)_6$-tagged fusion protein. A 2 ml starter culture of LB containing 100 µg/ml kanamycin was inoculated with a single colony of *E. coli* BL21(DE3) transformed with pET28-pfomt and incubated at 37 °C, 220 rpm for 6 hours. The main culture (N-*Z*-amine, *y*east extract, *p*hosphate (ZYP-5052) containing 200 µg/ml kanamycin) was inoculated with the starter culture such that OD^{600} was 0.05. The culture was incubated in a shaking incubator at 37 °C, 220 rpm over night (≈16 h). Due to the autoinducing nature of the ZYP-5052 medium, addition of IPTG was not neccesary. Cells were harvested by centrifugation at 10 000 × *g*, 4 °C for 10 min and the supernatant discarded. The pellet was resuspended in 50 mM Tris/HCl, 500 mM NaCl, 2.5 mM imidazole, 10 % glycerol pH 7 using a volume of ≈10 ml/g of cell pellet. The cells were lysed by sonication (70 % amplitude, 1 s on-off-cycle) for 30 seconds, which was repeated twice. The crude lysate was clarified by centrifugation at 15 000 × *g*, 4 °C for 15 minutes followed by filtration through a 0.45 µm filter. Consequently, the His-tagged PFOMT was purified by immobilized metal affinity chromatography (IMAC) (3.4.10). The eluted PFOMT protein was dialyzed (3.4.7) against 25 mM HEPES, 100 mM NaCl, 5 % glycerol pH 7 and stored at −20 °C until use.

Heterologous production of SOMT-2

SOMT-2 was produced as a fusion protein with an N-terminal His-tag. A starter LB-culture (≈ 2 ml) containing 100 µg/ml kanamycin was inoculated with a single colony of *E. coli* BL21(DE3) transformed with pET28MC-somt and incubated at 37 °C, 220 rpm for 6 hours. The starter culture was used to inoculate the main culture (LB-medium containing 100 µg/ml kanamycin), such that OD^{600} ≈ 0.05. The culture was incubated at 37 °C, 220 rpm in a shaking incubator until OD^{600}

BWEIGEL: Überprüfen!

≈ 0.6. Expression was induced by addition of 1 mM IPTG. Incubation continued at 37 °C, 220 rpm for 6 hours. Cells were harvested by centrifugation (10 000 × *g*, 4 °C, 10 min) and used, or stored at −20 °C until use. SOMT-2 was produced in inclusion bodies (IBs), which were prepared as laid out in subsection 3.4.9.

3.4.9 Preparation of inlusion bodies (IBs)

Often, when recombinant protein is produced in high levels in *E. coli* it is accumulated in so-called inlusion bodies (IBs) [88]. The accumulating IBs consist mainly of the overproduced target protein, which is inherently quite pure already. IBs can be selectively recovered from *E. coli* cell lysates and can consequently be refolded. IBs were prepared according to a modified protocol by Palmer [80].
The cells were resusupended in 5 ml/g_{cells} IB lysis buffer (100 mM Tris/HCl, 1 mM EDTA pH 7), 0.5 mM phenylmethylsulfonylfluoride (PMSF) was added as protease inhibitor. The solution was homogenized using a tissue grinder homogenizer (Ultra Turrax®; IKA®-Werke GmbH & Co. KG, Staufen, Germany). 200 µg/ml lysozyme was added to aid in the breakage of cells and the cells were lysed by sonicating thrice at 70 % amplitude (1 s on-off-cycle) for 30 seconds. DNase I (10 µg/ml) was added and the solution was incubated on ice for 10 min. The lysate was clarified by centrifuging for 1 h at 20 000 × *g*, 4 °C. The supernatant was discarded and the pellet was resuspended in 5 ml/g_{cells} IB wash buffer I (20 mM EDTA, 500 mM NaCl, 2 % (w/v) Triton X-100 pH), followed by thorough homogenization. The solution was centrifuged (30 min at 20 000 × *g*, 4 °C), the supernatant discarded and the pellet was washed twice more. To remove detergent, the pellet was washed twice again with IB washing buffer II (20 mM EDTA, 100 mM Tris/HCl pH 7). The IBs were resuspended in IB solubilization buffer (100 mM Tris/HCl, 5 mM DTT, 6 M GdmCl pH 7), such that the protein concentration was about 25 mg/ml and stored at −20 °C until use.

3.4.10 Purification of His-tagged proteins using immobilized metal affinity chromatography (IMAC)

N- or C-terminal oligo-histidine tags (His-tags) are a common tool to ease purification of recombinantly produced proteins. The free electron pairs of the imidazol nitrogens of histidines can complex divalent cations such as Mg^{2+} or Ni^{2+}, which are usually immobilized on a matrix of nitrilo triacetic acid (NTA)-derivatives. The affinity of the His-tag is correlated with its length and tagged proteins can simply be eluted by increasing the concentration of competing molecules (e.g. imidazole). His-tagged protein was purified by fast protein liquid chromatography (FPLC) via Ni^{2+}- (HisTrap FF crude) or Co^{2+}-NTA (HiTrap Talon FF crude) columns, obtained

from GE Healthcare (Freiburg, Germany), following modified suppliers instructions. First the column was equilibrated with 5 column volumes (CV) of binding buffer (50 mM Tris/HCl, 500 mM NaCl, 10 % glycerol, 2.5 mM imidazole pH 7). The sample (generally clarified lysate) was applied to the column using a flow of 0.75 ml/min. Unound protein was removed by washing with 3 CV binding buffer. Unspecifically bound proteins were washed away by increasing the amount of elution buffer (50 mM Tris/HCl, 500 mM NaCl, 10 % glycerol, 250 mM imidazole pH 7) to 10 % (constant for 3 to 5 CV). Highly enriched and purified target protein was eluted with 6 to 10 CV of 100 % elution buffer.

3.4.11 Refolding of SOMT-2 on a micro scale using design of experiments (DoE)

Design of experiments (DoE) and FFD have been successfully used to optimize the refolding conditions of several proteins [113, 3, 8]. Thus, an approach using FFD was used to find optimal refolding conditions for SOMT-2.
Factors studied were pH (buffer), arginine, glycerol, divalent cations, ionic strength, redox system, cyclodextrin and co-factor addition. The experimental matrix was constructed using the `FrF2` package (*http://cran.r-project.org/web/packages/FrF2/index.html*) in the R software.

Table 3.7.: Factors used in the construction of the FFD.

factor	symbol	setting		unit
		-1	+1	
pH	A	5.5	9.5	-
arginine	B	0	0.5	M
glycerol	C	0	10	% (v/v)
divalent cations[1]	D	no	yes	-
ionic strength[2]	E	low	high	-
redox state[3]	F	reducing	redox-shuffling	-
α-cyclodextrin	G	0	30	mM
SAH	H	0	0.5	mM

[1] no: 1 mM EDTA; yes: 2 mM $CaCl_2$, $MgCl_2$
[2] low: 10 mM NaCl, 0.5 mM KCl; high: 250 mM NaCl, 10 mM KCl
[3] reducing: 5 mM DTT; redox-shuffling: 1 mM glutathione (GSH), 0.2 mM glutathione disulfide (GSSG)

Table 3.8.: *Experimental design matrix for the FFD.*

Experiment	A	B	C	D	E	F	G	H
1	+	+	+	-	-	-	-	+
2	-	-	-	-	-	-	-	-
3	+	-	+	+	-	+	+	-
4	-	+	+	-	+	+	+	-
5	+	+	-	-	+	+	-	-
6	-	+	-	+	+	-	+	+
7	+	+	-	+	-	-	+	-
8	-	-	+	-	+	-	+	+
9	+	-	+	+	+	-	-	-
10	-	-	-	-	-	+	+	+
11	+	-	-	+	+	+	-	+
12	-	+	+	+	-	+	-	+

The buffers were mixed from stock solutions and prepared in 1.5 ml microcentrifuge tubes immediately prior to the experiment. 50 µl of solubilized SOMT-2 (1 mg/ml) in IB solubilization buffer was added to each buffer followed by a short vortex boost for rapid mixing. The final protein concentration in the refolding reaction was 50 µg/ml, whereas the remaining GdmCl concentration was ≈286 mM. The refolding reactions were incubated at RT for 1 hour, followed by an over night incubation at 4 °C. After incubation the refolding reactions were centrifuged (10 000 × g, 4 °C, 10 min) to separate insoluble and soluble protein fractions. The supernatant was transferred to a new tube, whereas the pellet was washed twice with 200 µl acetone and once with 400 µl methanol/acetone (1:1). The pellet was resuspended in 100 µl PBS with 20 µl SDS-PAGE sample buffer and 10 µl were used for SDS-PAGE analysis.

100 µl of the supernatant were concentrated using TCA precipitation (3.4.4) and analyzed by SDS-PAGE. The remaining supernatant was rebuffered into 50 mM 2-[Bis(2-hydroxyethyl)amino]-2-(hydroxymethyl)propane-1,3-diol (BisTris) pH 7.5 using Amicon® Ultra 0.5 ml centrifugal filters (Merck, Darmstadt, Germany) according to the manufacturers instructions. The pre-weighed collection tubes were re-weighed after recovery and the volume of recovered liquid calculated ($\rho \approx 1\,\mathrm{g/cm^3}$). The sample was filled up to 100 µl using 50 mM BisTris pH 7.5 and the protein concentration was assessed using the Roti®-Quant protein quantification solution (Carl Roth, Karlsruhe, Germany) according to the manufacturers description. 50 µl of each refolded sample was used for an activity test using naringenin as substrate (3.6.3). The reactions were incubated over night and stopped by the extraction method. However, before the actual extraction 1 µl of

anthracene-9-carboxylic acid (AC-9) was added as internal standard. The samples were analyzed by high-performance liquid chromatography (HPLC).

Assessment of refolding performance

The performance of each buffer on the refolding of SOMT-2 was examined by comparing the SDS-PAGE results, as well as the amount of soluble protein and the conversion of substrate. Main effects were analyzed qualitatively using main effects plots [12].

Upscaling of refolding reactions

Refolding reactions were scaled up to 50 ml. Therefore 2.5 ml solubilized SOMT-2 (1 mg/ml) were added over 10 minutes to 50 ml of refolding buffer while stirring at RT. The refolding reaction was allowed to complete over night at 4 °C.

3.4.12 Enzymatic production of SAM and SAE

SAM and *S*-adenosyl-L-ethionine (SAE) were prepared according to the method described by Dippe, et. al [22].
Preparative reactions (20 ml) were performed in 0.1 M Tris/HCl, 20 mM $MgCl_2$, 200 mM KCl pH 8.0 and contained 7.5 mM adenosine triphosphate (ATP), 10 mM D,L-methionine or D,L-ethionine, for the production of SAM or SAE respectively, and 0.2 U *S*-adenosylmethionine synthase (SAMS) variant I317V. The reaction was stopped by lowering the pH to 4 using 10 M acetic acid after 18 h of incubation at 30 °C, 60 rpm. After 10 min incubation on ice the solution was centrifuged (15 000 × *g*, 10 min) to remove insoluble matter. The supernatant was transferred to a round bottom flask, frozen in liquid nitrogen and lyophilized.
Crude products were extracted from the pellet using 73 % ethanol and purified using ion exchange chromatography (IEX). IEX was performed on a sulfopropyl sepharose matrix (25 ml) via isocratic elution (500 mM HCl). Before injection, the crude extract was acidified to 0.5 M HCl using concentrated hydrochloric acid. After elution, the product containing fractions were dried via lyophilization.
The amount of product was determined by UV/VIS-spectroscopy at 260 nm using the published extinction coefficient of SAM (ε_0 = 15 400 M^{-1} cm^{-1}) after resuspension in water [96].

3.5 Crystallographic Procedures

3.5.1 Crystallization of proteins

Commercially available crystallization screens were used to find initial crystallization conditions. The tested screens included kits available from Hampton Research (Aliso Viejo, USA) and Jena Bioscience (Jena, Germany). Crystallization screens were processed in 96-well micro-titer plate (MTP)s, where each well possessed 4 subwells aligned in a 2×2 matrix. The subwells were divided into 3 shallow wells for sitting drop vapour diffusion experimental setups and a fourth subwell, which was deep enough to act as buffer reservoir. This way the performance of each crystallization buffer could be assessed using three different protein solutions with varying concentrations, effectors etc. A pipetting robot (Cartesian Microsys, Zinsser-Analystik; Frankfurt, Germany) was used to mix 200 nl of each, protein and buffer solution, for a final volume of 400 nl. The crystallization preparations were incubated at 16 °C and the progress of the experiment was documented by an automated imaging-system (Desktop Minstrel UV, Rigaku Europe, Kent, UK). Furthermore, fine screens (e.g. for refinement of crystallization conditions) were set up by hand in 24-well MTPs using the hanging drop vapour diffusion method.

PFOMT

PFOMT protein was concentrated to (6 to 8) mg/ml and rebuffered to 10 mM Tris/HCl pH 7.5 using Amicon® Ultracel centrifugal concentrators (10 kDa MWCO). The concentrated protein solution was centrifuged at 14 000 × *g*, 4 °C for 10 min to remove any insoluble material or aggregates. Flavonoids and phenylpropanoid substrates were added to the protein solution from 10 mM stock solution in dimethyl sulfoxide (DMSO). Crystallization screens were set up as described above. *apo*-PFOMT was crystallized using the following conditions – 2 M $(NH_4)_2SO_4$, 20 %glycerol. The protein solution contained 0.25 mM SAE, 0.25 mM $MgCl_2$, 0.25 mM eriodictyol and 7.53 mg/ml (0.262 mM) PFOMT .

BWEIGEL: ist das korrekt?

Crystallization of proteins using NADES

NADES have the potential to be excellent solvents for hydrophobic compounds such as flavonoids or cinnamic acids [17] and in addition they are able to stabilize and activate enzymes [39].

BWEIGEL: To introduction

Four different model proteins (bovine trypsin, hen-egg white lysozyme, proteinase K and *Candida cylindrica* lipase B) were used to assess the capability of NADES for protein crystallization. PCH was tested in a full factorial grid layout using PCH concentrations of (20, 30, 40 and 50) % combined with buffers of different pH. The buffers included 0.1 M sodium acetate pH (4.5 and 5.5), 0.1 M sodium citrate pH 6.5, 0.1 M 2-[4-(2-hydroxyethyl)piperazin-1-yl]ethanesulfonic

acid (HEPES)/NaOH pH (7 and 7.5) and 0.1 M Tris/HCl pH 8.5. Thus, the full factorial design had a size of $4 \times 6 = 24$ different conditions. Protein solutions were prepared from lyophilized protein and were as follows: 90 mg/ml trypsin in 10 mg/ml benzamidine, 3 mM $CaCl_2$; 75 mg/ml lysozyme in 0.1 M sodium acetate pH 4.6; 24 mg/ml proteinase K in 25 mM Tris/HCl pH 7.5 and 6 mg/ml lipase B in water. For crystallization 2 µl enzyme solution and 1 µl reservoir buffer were mixed and set up in a hanging drop experiment on a 24-well MTP. The experiments were set up at 4 °C.

3.5.2 Data collection and processing

Crystallographic data were collected at the beamline of the group of Professor Stubbs (MLU, Halle, Germany). The beamline was equipped with a rotating anode X-ray source MicroMax007 (Rigaku/MSC, Tokio, Japan), which had a maximum power of 0.8 kW (40 kV, 20 mA) and supplied monochromatic Cu-K_α-radiation with a wavelength of 1.5418 Å. Diffraction patterns were detected with a Saturn 944+ detector (CCD++, Rigaku/MSC, Tokio, Japan).
Indexing and integration of the reflexes via Fourier transformation (FT) was accomplished using *XDS* [46, 45, 47] or *MOSFLM* [82]. *Scala* [27], which is integrated in the Collaborative Computational Project No. 4 (CCP4)-Suite, was used for scaling of the intensities.

3.5.3 Structure solution

For the determination of the electron density $\rho(\mathbf{r})$, where $\mathbf{r}$ is the positional vector, from the diffraction images by FT two terms are neccessary as coefficients; the *structure factor amplitudes*, $F_{\text{obs}}(\mathbf{h})$ and the *phase angles* or *phases*, $\alpha(\mathbf{h})$, where $\mathbf{h}$ is the reciprocal index vector. The structure factor amplitudes can be directly determined from the measured and corrected diffraction intensities of each spot. However, the phase information is lost during the detection of the diffracted photons and there is no direct way to determine the phases. This constitutes the so-called *phase problem*. Thus, additional phasing experiments are necessary in order to obtain the phases. A variety of phasing experiments are available, which include *marker atom substructure methods*, *density modification* and *molecular replacement (MR)* techniques [89]. Phases of the structures herein were exclusively determined by MR [86, 87].
MR was performed using the software *Phaser* [70, 71], which is included in the CCP4-Suite [115]. A previously published PFOMT structure (PDB-code: 3C3Y [52]) was used as a template during MR procedure for the PFOMT structure solution. For the MR of the lysozyme structure the PDB-entry 4NHI was used.

BWEIGEL: Lysozym struktur

3.5.4 Model building, refinement and validation

Macromolecular model building and manipulation, as well as real space refinement and Ramachandran idealization were performed using the Crystallographic Object-Oriented Toolkit (*Coot*) software [25]. Structure refinement was done using the software REFMAC5 [75, 107] as part of the CCP4-suite or the Phyton-based Hierarchial Environment for Integrated Xtallography (PHENIX) [1]. Validation of the structures was carried out using the web service MolProbity (*http://molprobity.biochem.duke.edu/*) [15]. Structure visualization and the preparation of figures was performed using PyMOL (Schrödinger, New York, USA).

3.5.5 *In silico* substrate docking

In silico molecular docking studies were performed using the AutoDock Vina 1.1.2 or AutoDock 4.2.6 software in combination with the AutoDockTools-Suite (*http://autodock.scripps.edu/*) [40, 73, 106]. Substrates were docked into the PFOMT structure with the PDB-code 3C3Y. The grid box, which determines the search space, was manually assigned to center at 1.581, 5.196 and 25.718 (x, y, z) and had size of (22, 20 and 25) Å (x, y, z). The exhaustiveness of the global search for AutoDock Vina was set to 25, whereas the rest of the input parameters were kept at their defaults.

3.6 Analytics

3.6.1 Recording of growth curves

Starter cultures (≈2 ml) of the transformed *E. coli* cells were prepared in the medium to be studied, containing the appropriate antibiotics. The cultures were incubated at 37 °C, 200 rpm over night and harvested by centrifugation (5000 × *g*, 4 °C, 5 min). The pellet was resuspended in 15 ml PBS and the suspension centrifuged (5000 × *g*, 4 °C, 5 min). The supernatant was discarded and the washing step repeated once more. The washed pellet was resuspended in 2 ml of the medium to be studied with the appropriate antibiotics and the OD^{600} was measured. Three independent 50 ml cultures of the medium containing the appropriate antibiotics were inoculated such that $OD^{600} \approx 0.05$ using the washed cell suspension. The cultures were incubated at the conditions to be studied and sampled at appropriate intervals of time (≈1 h). One ml samples were kept on ice until all samples were aquired. 100 µl aliquots of the samples were transferred into a clear MTP and the OD^{600} was measured. Green fluorescent protein (GFP) fluorescence was measured accordingly, but the

MTP used was opaque. Exitation (λ^{ex}) and emission (λ^{em}) wavelengths were (470 and 510) nm respectively.

3.6.2 *In vitro* determination of glucose

The glucose concentration in clarified, aqueous samples was determined by a modified version of the glucose assay kit procedure provided by Sigma-Aldrich [98]. Glucose oxidase (GOD) oxidizes D-glucose to gluconic acid, whereby hydrogen peroxide is produced. The hydrogen peroxide can be detected and quantified by horseradish peroxidase (HRP), which reduces the produced H_2O_2 and thereby oxidizes its chromogenic substrate *o*-dianisidine via consecutive one-electron transfers. The oxidized diimine form of *o*-dianisidine can then be measured photospectrometrically [16].
The methodology employs a coupled photospectrometric assay using GOD and HRP with *o*-dianisidine as reporter substrate. The assay was prepared in MTP-format. A reaction solution containing 12.5 U/ml GOD, 2.5 U/ml HRP and 0.125 mg/ml *o*-dianisidine dihydrochloride in 50 mM sodium acetate pH 5.1 was prepared.
Sample solutions from culture supernatants were typically diluted in 9 volumes of water. The reaction was started, by adding 50 µl reaction solution to 25 µl of sample and was incubated at 37 °C and 200 rpm for 30 min in a shaking incubator. 50 µl 6 M sulfuric acid was added to stop the reaction and achieve maximum color development (full oxidation of any *o*-dianisidine charge transfer complexes) (Figure 3.1). The developed pink color was measured at 540 nm in a MTP-reader. A calibration curve of a standard D-glucose solutions (0 to 100 µg/ml), that was always part of the experiments, was used to quantify the sample measurements.

3.6.3 *In vitro O*-methyl transferase (*O*-MT) assay

O-methyl transferase (*O*-MT) assays were conducted in a total volume of (50 to 100) µl. The standard assay buffer was 100 mM Tris/HCl, 2.5 µM GSH pH 7.5. 1 mM $MgCl_2$, which was otherwise omitted, was added for reactions using cation dependent *O*-MTs (e.g. PFOMT). Reactions contained 0.5 mM alkyl donor (e.g. (*S*,*S*)-SAM) and 0.4 mM flavonoid or cinnamic acid substrate. Enzymatic reactions were started by addition of enzyme (usually 0.2 mg/ml) and incubated at 30 °C.

BWEIGEL: nochmal auseinanderklamüsern wegen den konzentrationen und eingesetzten enzymmengen...

Reactions were stopped by addition of 500 µl ethyl acetate containing 2 % formic acid and vortexed for 15 s to extract the hydrophobic phenylpropanoids and flavonoids. After centrifugation (10 000 × *g*, 4 °C, 10 min) the organic phase was transferred into a new tube. The reaction was extraced once more with 500 µl ethyl acetate, 0.2 % formic acid and the pooled organic phases were evaporated using a vacuum concentrator (Concentrator 5301; eppendorf, Hamburg, Germany). The residue was

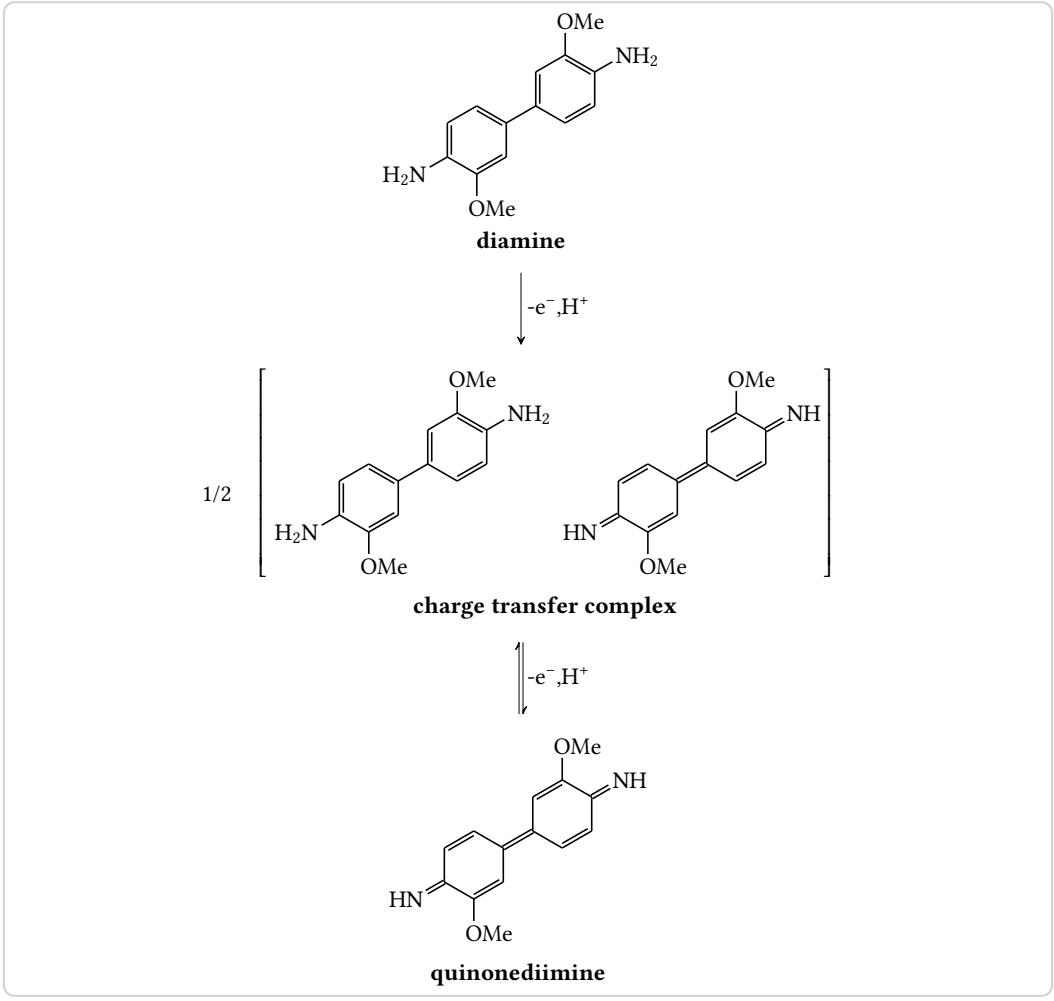

Figure 3.1.: *Oxidation of the reporter substrate o-dianisidine. Consecutive one-electron transfers lead to the fully oxidized diimine form of o-dianisidine. The first electron transfer is believed to produce a charge transfer complex intermediate. [44, 16]*

dissolved in methanol and centrifuged at 10 000 × *g* for 10 min to remove unsoluble matter. The supernatant was transferred into a HPLC vial and analyzed by HPLC (3.6.8).

When detection of hydrophobic (e.g. flavonoids) and hydrophilic compounds (e.g. SAM, SAH) was performed simultaneously reactions were stopped by addition of 0.3 volumes 10 % (w/v) TCA in 50 % acetonitrile. The mixture was vortexed for complete mixing and incubated on ice for at least 30 min. After centrifugation (10 000 × *g*, 4 °C, 10 min) the supernatant was transferred into HPLC-sample vials and analyzed (see 3.6.8).

Measurement of activity/pH profiles

Assays to measure activity over larger pH ranges were set up in 50 mM L-malic acid/MES/Tris (MMT)- (pH 4 to 9) or succinate/sodium phosphate/glycine (SSG)-buffer (pH 4 to 10) to keep the concentrations of buffer salts constant for each pH [76].

The protein of interest was first extensively dialyzed against the reaction buffer (e.g. MMT, SSG) at pH 7 with added EDTA (5 mM) and then against the same buffer without EDTA. Standard reaction conditions were 50 mM buffer, 0.4 mM alkyl acceptor (e.g. caffeic acid), 0.5 mM SAM, 2.5 µM GSH and 0.2 mg/ml enyzme. $MgCl_2$ was either omitted or added at 10 mM to assess influences of divalent cations. Assays were stopped as described in 3.6.3 and analyzed accordingly.

3.6.4 Photospectrometric assay for the methylation of catecholic moieties

Catecholic moieties can form stable complexes in the presence of heavy metals such as copper or iron [95, 72]. Hence, caffeic acid can complex ferric (Fe^{3+}) ions and form a colored complex with λ_{max} = 595 nm [21]. Since the complex formation is specific for caffeic acid and methylated derivatives (i.e. ferulic and iso-ferulic acid) cannot complex Fe^{3+}, this can be used as a measure for methylation reactions. *O*-MT assays were prepared as before (3.6.3). However, the reactions were stopped by addition of 0.1 volumes 1 M Tris/HCl pH 8, immediately followed by 0.5 volumes catechol reagent (2 mM $FeCl_3$ in 10 mM HCl). The complex formation reaction was allowed to equilibrate for 5 min at RT and the absorbance at 595 nm was measured.

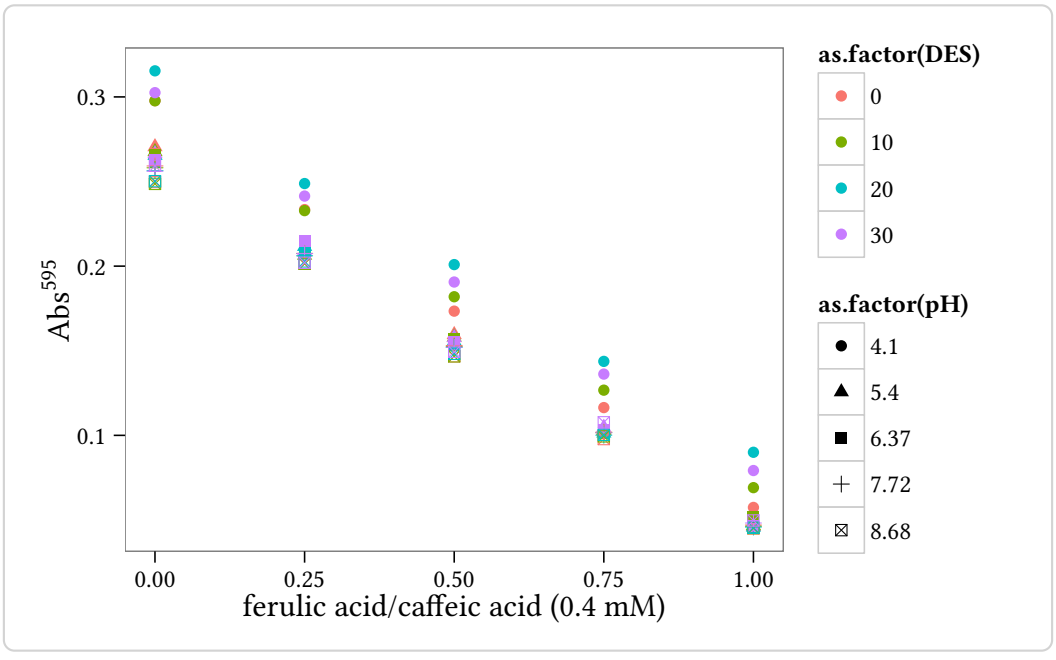

Figure 3.2.: *Calibration curves of different relative compositions of ferulic acid to caffeic acid, that were taken as described in 3.6.4. The total concentration was always* 0.4 mM. *At lower pH values around 4, the method seems to overestimate the concentration of caffeic acid. However, the slope of the curves stays the same.*

3.6.5 Concentration of SOMT-2 using hydrophobic interaction chromatography (HIC)

After refolding using rapid dilution protein samples are very dilute and a concentration step is required. Refolded SOMT-2 was concentrated directly from the refolding buffer using hydrophobic interaction chromatography (HIC).
The ammonium sulfate concentration of the protein sample was brought to 1 M using a 2 M $(NH_4)_2SO_4$ solution and the pH was adjusted to 7 using 5 M NaOH. The sample was centrifuged (20 000 × g, 4 °C, 30 min) to remove insoluble material and the clarified supernatant was applied to a 1 ml HiTrap Phenyl FF (Low Sub) (GE Healthcare, Freiburg, Germany), which had been equilibrated with high salt buffer (1 M $(NH_4)_2SO_4$, 50 mM HEPES pH 7). The target protein was eluted using a stepwise gradient ((1, 0.8, 0.6, 0.4, 0.2 and 0) M $(NH_4)_2SO_4$, 50 mM HEPES pH 7; 5 CV each) to remove the ammonium sulfate. The column was washed using 20 % ethanol. Before SDS-PAGE analysis the eluted high salt fractions were desalted using TCA precipitation (3.4.4).

3.6.6 Analytical gel filtration

Analytical gel filtration was done using a Superdex 200 10/300 GL column (GE Healthcare, Freiburg, Germany) in combination with a FPLC system according to the manufacturers instructions. The column was equilibrated using an appropriate buffer (e.g. 0.1 M Tris/HCl pH 7.5) and 100 µl of sufficiently concentrated (≥1 mg/ml) protein sample were injected. The Gel Filtration Standard by Bio-Rad (München, Germany) was run seperately to assess the size of the proteins in the analyzed sample.

3.6.7 Binding experiments using Isothermal Titration Calorimetry (ITC)

Isothermal Titration Calorimetry (ITC) can be used to directly characterize the thermodynamics of an observed process, be this a binding interaction or an enzymatic reaction [28].
ITC measurements to describe the interaction between PFOMT and its substrates/-effector where performed using a MicroCal iTC200 device (Malvern, Worcestershire, UK). PFOMT protein was extensively dialyzed against 50 mM MMT-buffer pH 7 prior to ITC experiments. The solution was susequently centrifuged (14 000 × g, 4 °C, 10 min), to remove insoluble matter and aggregates. The dialysate was stored at 4 °C and used to prepare substrate and effector solutions. Generally 50 µM protein was provided in the ITC cell and the effectors/substrates to be titrated were loaded

into the syringe. The substance concentration in the syringe was ten times higher than the protein solution. Experiments were carried out at 20 °C unless otherwise stated. The stirring speed was set to 500 rpm. The injection volume was set to (2 to 4) µl, amounting to a total of 10 to 19 injections.

3.6.8 High-performance liquid chromatography (HPLC) analytics

Due to their aromaticity, methanolic extracts of flavonoids exhibit two major absorption peaks in the UV/VIS region of the light spectrum in the range of (240 to 400) nm [64]. However, even the more simple phenyl propanoids (e.g. cinnamic acids) show absorption of light in the UV/VIS-region.
Methanolic extracts of flavonoids and phenyl propanoids were analyzed by HPLC using a photo diode array (PDA)-detector, which was set to record in the range of (200 to 400) nm. HPLC runs were performed on a reverse-phase C-18 end-capped column (YMC-Pack ODS-A; YMC Europe, Dinslaken, Germany) with a pore size of 120 Å. The mobile phase was aqueous acetonitrile supplemented with 0.2 % formic acid. The flow was kept constant at 0.8 ml/min. 10 µl *O*-MT enzyme assay extract (3.6.3) were injected and analyzed using an acetonitrile gradient starting with 5 % acetonitrile (4 min). The acetonitrile content was increased to 100 % in 21 min and was kept at 100 % for 5 min. Peaks were integrated from the 280 nm trace using the software provided by the manufacturer of the device.

3.6.9 liquid chromatography coupled mass-spectrometry (LC/MS) measurements

4 Evaluation of PFOMT towards the acceptance of long-chain SAM analogues

4.1 Introduction

Small changes to molecules can have profound influences on their chemical, physical and biological properties. Butyric acid esters differing only by a few methylene groups already exhibit quite divergent smells. However, not only the macroscopically qualitative properties can differ. The quantifyable psychotomimetic effect of methylated and ethylated lysergic acid amids differ by at least an order of magnitude [97, 37]. There are many more of these so-called structure activity relationships (SARs) and quantitative structure activity relationships (QSARs) studies on any number of compounds and situations [92, 4, 67].

Methylation reactions are one of the key tailoring steps during natural product biosynthesis and can in consequence greatly affect a molecules bio- and physicochemical behavoir [102, 57]. However, between the highly complex core structures of natural products, which are produced by a plethora of enzymes (e.g. poly ketide synthases (PKSs), non-ribosomal peptide synthases (NRPSs), terpene cyclases), and the rather simple alkyl-modification introduced by methylation nature is missing some medium-sized modifaction options, that proceed as elegantly as the methylation by MTs. Thus, natural products containing longer chain alkyl modifications like ethyl or propyl moieties on O, N or S-centers have rarely, if ever been observed.[1]

It has recently been shown however, that a wide array of SAM analogues are used as co-substrates by a variety of MTs [102]. The majority of the work so far has been done on P-MTs and DNA MTs (Figure 4.1), since epi-genetics and finding

[1] Reaxys searches for natural product isolates with a molecular mass between (150 and 1500) containing the substructures methyl, ethyl or propyl connected to a heteroatom return 66759, 2797 and 52 results respectively. However, it stands to note that 70 % of the propyl results were either esters or otherwise activated moieties. [24]

regions of gene-reulation is of great interest. There have been a great many of SAM analogues synthesized, both chemically and with the help of enzymes [18, 99].

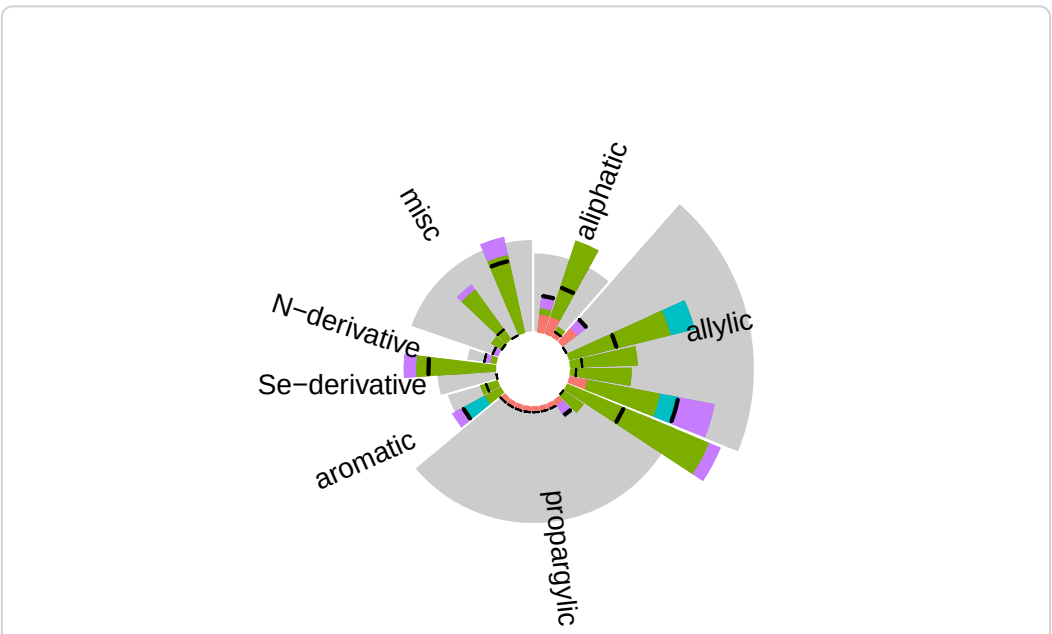

Figure 4.1.: *Graphical representation of the work that has been done on MTs in combination with SAM analogues. The grey areas represent individual groups of SAM analogues (aliphatic, allylic, propargylic, aromatic, SeAM analogues, nitrogen analogues and miscelaneous others). The height of the grey areas represents the number of times a member of the corresponding group has been described as tested in the MT literature. The height of the colored bars represents the times that individual substrate has been tested. The colors represent the different types of MT (red – DNA MT, green – P-MT, lilac – small molecule MT, blue – rna MT). The black dash across the bar shows the number of times this substrate was actually converted by either enzyme.*

However, the first description of novel synthetic SAM analogues with extended carbon chains, including SAE, allyl and propargyl derivatives, that were also shown to be useful in modifying DNA via the action of several DNA MTs was provided by Dalhoff, *et al.* [18, 19]. It was also noted, that allyl transalkylation reactions proceeded much faster than ethyl- or propyl transfers possibly due to conjugative stabilization of the transition state [18]. A whole variety of allyl derivatives was examined by different researchers and site-specific introductions of allyl, pent-2-

en-4-ynyl and even 4-propargyloxy-but-2-enyl moieties into proteins (i.e. histones) was demonstrated using P-MTs [112, 81]. However, the larger substrate analogues were not neccesarily accomodated by the native P-MTs making engineering efforts for the accomodation of larger substrates inevitable [112]. The specific introduction of alkine functionalized groups made it then possible to use click chemistry for further functionalization and/or detection of the labelled proteins, DNA or RNA and has been studied extensively (Figure 4.2) [112, 81, 74, 114, 93].
In 2012 Bothwell and Luo even described the exchange of the sulfonium with a selenonium center, which afforded *Se*AM analogues that have since then been described as substrates for several P-MTs [11, 10]. *Se*AM analogues have the advantage of being more resistant to chemical decomposition than their sulfur counterparts, but also show enhanced transmethylation reactivity [10].

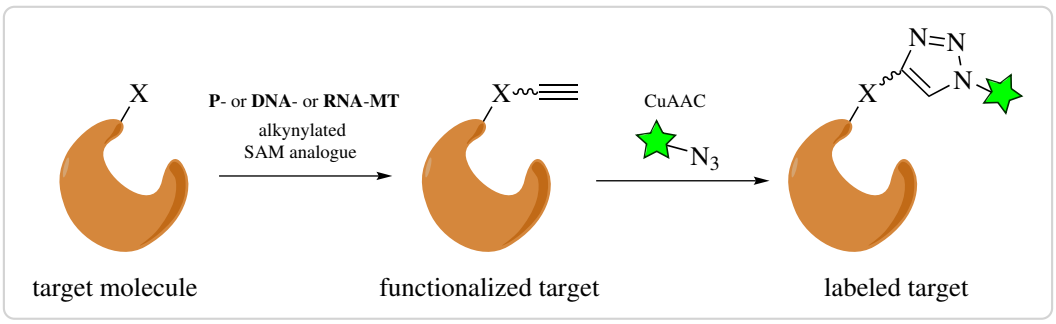

Figure 4.2.: *Labelling of macromolecules by using a combination of novel alkine-derivatized SAM analogues and Cu^{I}-catalyzed azide-alkyne 1,3-dipolar cycloaddition (CuAAC). Depending on the type of label used, it can be employed for detection (e.g. through fluorophores, coupled assays) or affinity purification (e.g. biotin). This technique is also feasable for use in activity based protein profiling (ABPP) approaches.*

There have also been some reports on the use of SAM analogues by small molecule MTs. In 2009 Stecher *et al.* reported the use of the *C*-methyl transferases (*C*-MTs) NovO and CouO along with synthetic SAM analogues to accomplish biocatalytic Friedel-Crafts alkyations of some aminocoumarine antibiotics [100]. Lee *et al.* were the first ones to describe the transfer of a keto-group from an SAM derivative by means of the small molecule MTs catechol *O*-methyl transferase (EC 2.1.1.6) and thiopurine *S*-methyl transferase (EC 2.1.1.67) [56]. Furthermore there was work done on the *O*-MTs RebM and RapM, which modify the antitumor active natural products rebeccamycin and rapamycin respectively, that shows the general feasability of using SAM analogues in combination with MTs to modify small molecules [55, 99, 118]. In all of these reports the specificity of the group transfer is retained despite the fact that SAM analogues are employed as substrates.

There is of yet no bioactivity data reported that shows the biological activity of the newly produced compounds.

PFOMT is highly promiscuous towards its flavonoid substrate [52, 41]. However, the promiscuity towards different SAM analogues has net yet been described. Combination of both, substrate and co-substrate promiscuity in the small molucule MT PFOMT could provide a powerful tool towards the biosynthestic production of novel small molecules with potentially new and promising biological activities. Functionalization/Detection of substrates could furthermore provide a means of finding new compounds/substrates in complex (e.g. biological) samples analogous to activity based protein profiling (ABPP) approaches. It was thus of interest, whether or not PFOMT would accept SAM analogues as alkyl donors. The already extensively studied PFOMT was the prime candidate, since the preparation and crystallizability were established and lots of substrates had already been described [**Brandt2015**, 108, 41, 52].

4.2 Substrate binding studies using ITC

The binding of different substrates by PFOMT was examined by ITC. SAH, SAM and SAE were selected to study the influence of the alkyl chain length on binding. Furthermore the binding of the substrate caffeic acid and the influence of Mg^{2+} addition on substrate binding was investigated.

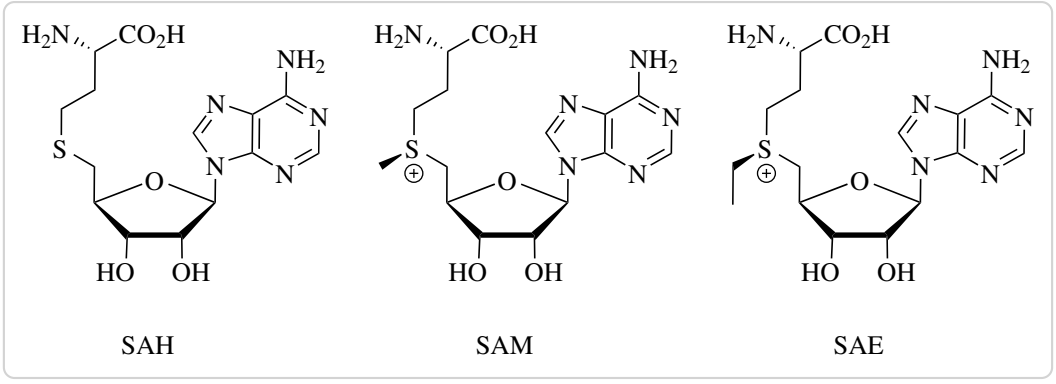

Figure 4.3.: *The binding of*

4.3 Study of variants for long-chain alkylations

The work described in this section was done in cooperation with Dr. Martin Dippe. Dr. Dippe did most of the work on the PFOMT variants described herein.

Since the ability to bind the enlongated analogue SAE was present in wildtype PFOMT, the activity of the PFOMT protein was tested. Activity tests were performed with caffeic acid as substrate under standard reaction conditions. The wildtype of PFOMT was able to use SAE as a co-substrate for the ethylation of caffeic acid, albeit the amount of detected product was very minute. The site of ethylation was determined by liquid chromatography coupled mass-spectrometry (LC/MS) measurements. It was found that ethylation occurs on the catecholic group, however it could not be determined whether at the 3- or 4-position. Nonetheless it is highly likely that ethylation occurs at the same position as methylation and thus the product was annotated as 3-ethoxy-4-hydroxy cinnamic acid.

BWEIGEL: literaturvergleich der umsäzte?

BWEIGEL: LCMS messungen?

Enzyme variants were prepared to further test the ethylation reactivity of PFOMT, since a number of groups were able to accomplish transalkylation with larger substrates by expanding the available space in the active site [112]. Residues that were exchanged were selected based upon their position in the active site and in relation to the substrate(s) (Figure 4.4). Fortunately a crystal structure of PFOMT was available to help with the selection.

BWEIGEL: Genauer zu den Resten...

Over 20 enzyme variants were prepared to assess, whether PFOMT ethylation activity would improve over the wildtype. Be that as is may, an improved ethylation activity was not observed. Some of the new variants however displayed an increased methylation activity with the substrates caffeic acid and SAM. The methylation activity of some of the variants increased by over 4-fold . Interestingly most amino acid substitutions proved as beneficial, rather than detrimental.

BWEIGEL: grafik?

Methylation activity benifited greatly from the replacement of bulky hydrophobic residues by smaller and/or charged residues in the vicinity of the acceptor substrates (Tyr51, Trp184 and Phe198). However, this was not a general trend since the substitutions N202W and Y51W also improved methylation activity. Looking more closely at residue Tyr51, the activity enhancing effect was greatest, when the tyrosine was substituted by the basic amino acids lysine or arginine. In addition to an enhanced activity the selectivity for the hydroxyl position to be methylated was also altered in these variants. This was not apparent, when caffeic acid was used as a substrate. However when a flavonoid, especially eriodictyol, was used not only the 3' hydroxyl, but to some extent the 4' hydroxyl was methylated. This effect was improved in some double variants, where also position 202 was altered. For example the variant Y51R N202W almost exclusively methylated flavonoid

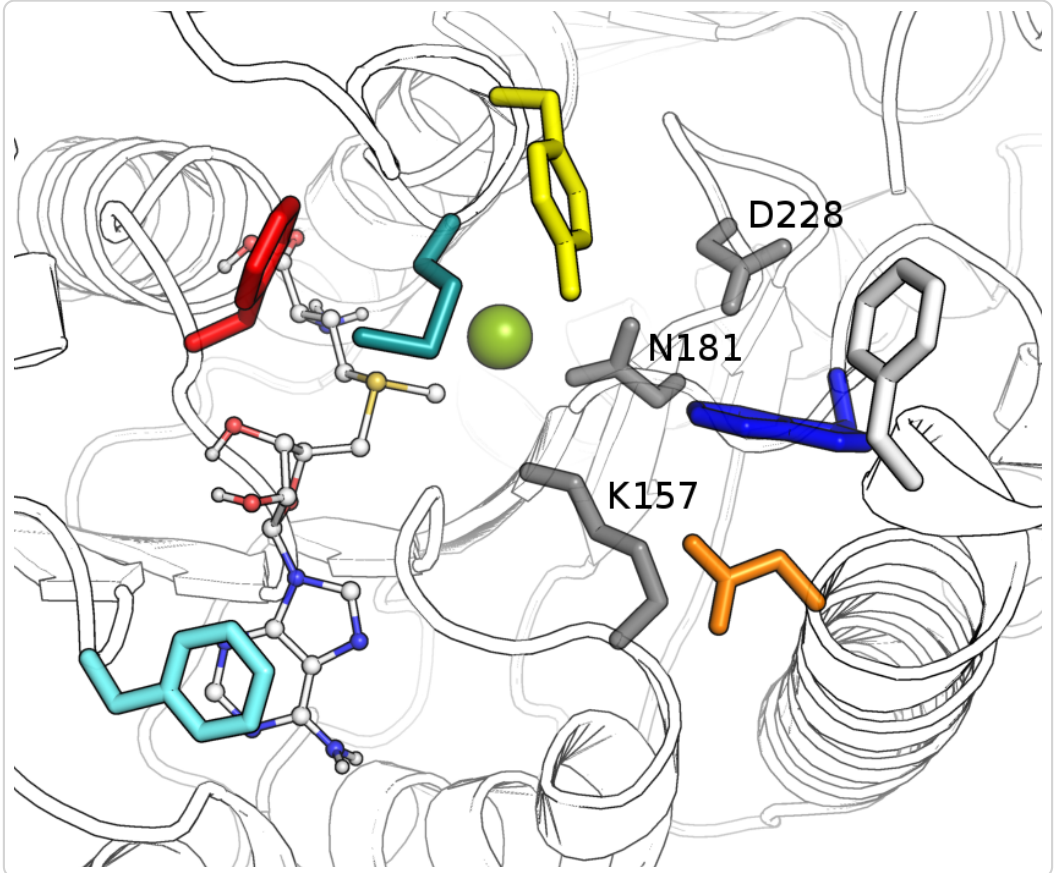

Figure 4.4.: *The active site of PFOMT. The outline of the protein backbone is displayed, with active site residues portrayed as colored sticks (cyan – F103, red – F80, turquoise – M52, yellow – Y51, white – F198, blue – W184, orange – N202, grey – as labelled). The co-substrate SAM (ball-and-stick model) was docked into the structure.*

substrates at the 4' position . A detailed discussion of the results was published in a peer reviewed journal.

BWEIGEL: grafik? & paper

4.4 Crystallization of PFOMT

The binding of the non-natural substrate SAE to PFOMT could be shown. However, a transethylation reactivity was not observed. The question was to the chemical reasons behind these observations. Previous work on the crystal structure of PFOMT had been done, but only SAH could be co-crystallized [52]. But since the crystallizability of PFOMT had already been shown, this method was chosen to answer the aforementioned question.

At first the already crystallization procedures were evaluated to start with [52]. Albeit, reproduction of the results could not be accomplished and new crystallization conditions had to be found. This was done using commercially crystallization screening kits and a semi-automated pipetting robot along with an automated imaging system for the observation of the crystallization plates.

Each buffer solution was screened in combination with three different protein solutions (*A* – 0.25 mM SAH, 0.25 mM $MgCl_2$, 0.25 mM ferulic acid, 0.262 mM PFOMT; *B* – 0.25 mM SAE, 0.25 mM $MgCl_2$, 0.25 mM eriodictyol, 0.262 mM PFOMT and *C* – 0.25 mM SAH, 0.25 mM $MgCl_2$, 0.25 mM ferulic acid, 0.219 mM PFOMT Y51R N202W) to obtain protein crystals co-crystallized with the substrates.
During the preparation of the protein solutions it was noted, that upon addition of the flavonoids or phenyl propanoids from DMSO stocks these tended to precipitate. Thechniques meant to circumvent this problem are discussed in chapter 7. Crystals began to appear in various wells after a few days and were observed for each tested protein solution at least once. The crystal shape varied from very smooth and almost cubic (high ammonium sulfate) over sphreulites and intergrown crystals ($CaCl_2$, PEG-4000) to brittle and ragged needles (LiCl, PEG-6000) (Figure 4.5).

Crystals that were large enough (≥ 50 µm), where screened for diffraction right away. A rough estimate of the resolution, cell parameters and the space group was aquired, if the diffraction images could be indexed. The screened crystals all had similar cell parameters and belonged to the same space group, $P2_12_12_1$. However, the unit cell of crystals that grew out of high ammonium sulfate concentrations (≥1.8 M) was approximately four times as large as that of the published structure 3C3Y and crystrals that developed under different crystallization conditions. Consequently the assymetric unit consisted of 4, instead of 2 PFOMT monomers. Several datasets were collected of crystals from high $(NH_4)_2SO_4$, since these possessed different cell parameters than the previously reported structure and therefore seemed to be promising candidates for bound substrates.

BWEIGEL: wie groß?

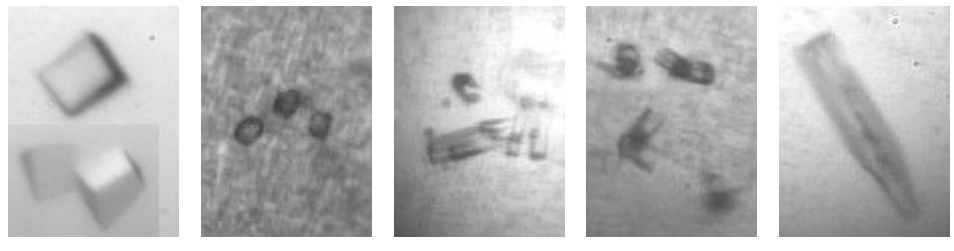

(a) *(b)* *(c)* *(d)* *(e)*

Figure 4.5.: *Some crystal and pseudo-crystal shapes that were observed during the crystallization screen. a – high $(NH_4)_2SO_4$, b-c – $CaCl_2$, PEG-4000, e – LiCl, PEG-6000*

The crystal structure of *apo*-PFOMT

Most of the collected datasets were partly solved. As it turned out however the substrates were not co-crystallized. Rather, the *apo*-form of PFOMT had been crystallized. Thus, one dataset was solved to completion to obtain a novel PFOMT structure with no substrate bound.

The assymetric unit of *apo*-PFOMT contained two homodimers (4 monomers). The active site of each monomer was found to be empty except for a sole sulfate ion, which was positioned where the amino- and carboxylate group of the SAH reside in the 3C3Y structure. Significant shifts in the structure of some loops were observed and contrary to the previously published structure the N-terminus of the monomers was resolved up to the His-tag.

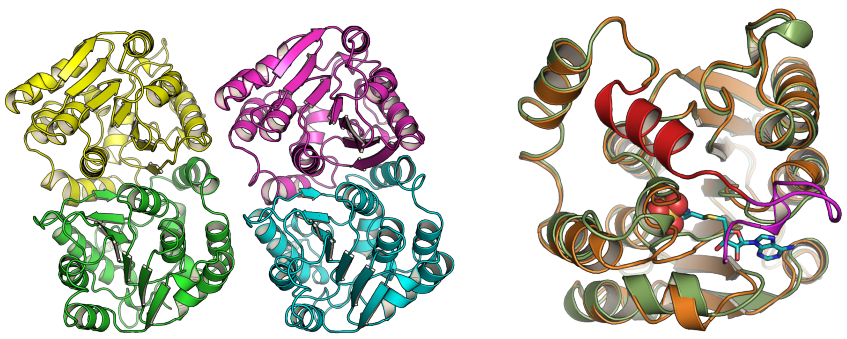

(a) *assymetric unit* *(b)* *comparison of 3C3Y and* apo*-PFOMT*

Figure 4.6.: *An overview of the features in the* apo*-PFOMT structure.*

Table 4.1.: *Crystallographic data, phasing and refinement statistics.*

	140519_PFOMT	MC001413-G10.1
data collection		
wavelength (Å)		
resolution (Å)	1.95	
total reflections	392 368	
unique reflections	125 822	
completeness (%)	99.12	
$I/\sigma(I)$	9.9	
R^a_{sym}		
redundancy		
space group	$P2_12_12_1$	
cell dimensions (Å)		
a	86.16	48.88
b	128	71.36
c	129.3	127.80
refinement		
R_{work}/R_{free}	0.21369 / 0.24700	
rmsd bond lengths (Å)	0.0199	
rmsd bond angles (°)	2.0568	
B-values (Å^2)	21.593	
water		
ions		
Ramachandran plot (%)		
favoured	96.82	
allowed	2.38	
outliers	0.8	

4.4.1 PFOMT activity in deep eutectic solvents (DES) / Solubility-enhancing effects of DES

vielleicht eigenes kapitel DES?

4.4.2 PFOMT-Paper (DIM)

4.4.3 Dockings???

4.5 Conclusion/Discussion

5 Enzymatic methylation of Non-catechols

5.1 Introduction

Non-catechols in nature (biosynthesis, mode of action?), chemical methylation???

5.2 SOMT-2

5.2.1 In vivo methylation studies using *N. benthamiana*

5.2.2 In vivo studies in *E. coli*

5.2.3 In vitro studies using recombinantly produced SOMT-2

5.3 PFOMT

5.3.1 Acidity and Nucleophilicity of phenolic hydroxyl-groups

5.3.2 pH-Profiles of PFOMT-catalysis

5.3.3 Influence of Mg^{2+} on PFOMT activity

5.4 Consensus or Bioinformatic points-of-view (COMT)???

5.5 Conclusion/Discussion

6 Development of an whole cell methyl transferase screening system

6.1 Introduction

6.2 Theoretical considerations / design of system

6.3 Detectability of *S*-adenosyl-L-homocysteine (SAH)

SAM

6.4 Usage of the lsr-promoter for true autoinduction

6.5 Conclusion/Discussion

7 DES in protein crystallography

7.1 Introduction

7.2 Solubility enhancement of hydrophopbic substances by addition of DES

7.3 Enzymatic *O*-methylation in DES

7.4 DES as precipitants in protein crystallization

7.5 Conclusion/Discussion

8 Acknowledgements

Quisque ullamcorper placerat ipsum. Cras nibh. Morbi vel justo vitae lacus tincidunt ultrices. Lorem ipsum dolor sit amet, consectetuer adipiscing elit. In hac habitasse platea dictumst. Integer tempus convallis augue. Etiam facilisis. Nunc elementum fermentum wisi. Aenean placerat. Ut imperdiet, enim sed gravida sollicitudin, felis odio placerat quam, ac pulvinar elit purus eget enim. Nunc vitae tortor. Proin tempus nibh sit amet nisl. Vivamus quis tortor vitae risus porta vehicula.

Fusce mauris. Vestibulum luctus nibh at lectus. Sed bibendum, nulla a faucibus semper, leo velit ultricies tellus, ac venenatis arcu wisi vel nisl. Vestibulum diam. Aliquam pellentesque, augue quis sagittis posuere, turpis lacus congue quam, in hendrerit risus eros eget felis. Maecenas eget erat in sapien mattis porttitor. Vestibulum porttitor. Nulla facilisi. Sed a turpis eu lacus commodo facilisis. Morbi fringilla, wisi in dignissim interdum, justo lectus sagittis dui, et vehicula libero dui cursus dui. Mauris tempor ligula sed lacus. Duis cursus enim ut augue. Cras ac magna. Cras nulla. Nulla egestas. Curabitur a leo. Quisque egestas wisi eget nunc. Nam feugiat lacus vel est. Curabitur consectetuer.

III

Appendix

A Figures

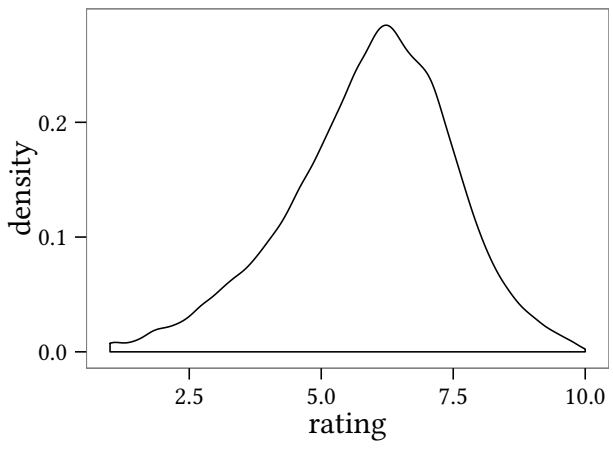

Figure A.1.: *Lorem ipsum dolor sit amet, consectetuer adipiscing elit. Aenean commodo ligula eget dolor. Aenean massa. Cum sociis natoque penatibus et magnis dis parturient montes, nascetur ridiculus mus. Donec quam felis, ultricies nec, pellentesque eu, pretium quis, sem.*

B Tables

Table B.3.: SAM analogues that have been used with MTs. Targets: P *– peptide/protein,* D *– DNA,* R *– RNA,* S *– small molecule.*

analogue	enzyme	target	references
SAM			
$-CH_2-CH_3$	PRMT1, M.TaqI, M.HhaI, M.BcnIB, RebM, RapM	S,P,D	[105, 18, 99, 55] [1]
$-CH_2-CH_2-CH_3$	PRMT1, M.TaqI, M.HhaI, M.BcnIB	P,D	[105, 18]
$-CH_2-CH_2-CH_2-CH_3$	PRMT1	P	[105]
$-CH_2-C_6H_5$	NovO, CouO, PRMT1	S,P	[100, 105]
$-CH_2-C(=O)-CH_3$	COMT, TPMT, CazF	S	[56, 116]
$-CH_2-CH=CH_2$	NovO, CouO, RapM, PRMT1, M.TaqI, M.HhaI, M.BcnIB, RebM, Tgs	P,S,D	[100, 105, 18, 99, 112, 111, 104, 55, 93]
$-CH_2-CH=CH-CH_3$	NovO, CouO	S	[100]

[1] Singh *et al.* (2014) published a series of 44 biocatalytically synthesized SAM and *Se*AM derivatives, most of which were not tested towards their alkyl donation potential in MT reactions.

Appendix B. Tables

analogue	enzyme	target	references
$-CH_2-C\equiv CH$	Dim-5, *Hs*MLL, TRM1, NovO, CouO, PRMT1	P,R,S	[114, 100, 112, 111, 43]
$-CH_2-C\equiv N$	RebM	S	[99]
$-CH_2-CH_2-C\equiv CH$	PKMT	P	[43]
$-CH_2-CH_2-CH_2-C\equiv CH$	PKMT	P	[43]
$-CH_2-C\equiv C-CH_3$	NovO, CouO, M.HhaI, M.TaqI, M.BcnIB	S,D	[100, 18, 62]
$-CH_2-C\equiv C-CH_2-CH_3$	M.HhaI	D	[62]
$-CH_2-C\equiv C-CH_2-NH_2$	M.HhaI	D	[62]
$-CH_2-C\equiv C-CH_2-NH-C(=O)(-CH_2-)_3-NH_2$	M.HhaI	D	[62]
$-CH_2-C\equiv C(-CH_2-)_3-NH_2$	M.HhaI	D	[62]
$-CH_2-C\equiv C(-CH_2-)_3-NH-C(=O)(-CH_2-)_3-NH_2$	M.HhaI	D	[62]
$-CH_2-C\equiv C(-CH_2-)_3-C\equiv CH$	M.HhaI	D	[62]
$-CH_2-C\equiv C(-CH_2-)_3-N_3$	M.HhaI	D	[62]
$-CH_2-CH=CH-C\equiv CH$	Dim-5, *Hs*MLL, TRM1, PRMT1, Tgs	P,R	[114, 81, 112, 111, 74, 43, 93]
$-CH_2-CH=CH-CH_2-C\equiv CH$			[111, 43]
$-CH_2-CH=CH-CH_2-O-CH_2-C\equiv CH$	PRMT1	P	[112, 111]
SeAM			
$-CH_3$			
$-CH_2-C\equiv CH$	Dim-5, *Hs*MLL, TRM1, RebM, CazF	P,R,S	[114, 99, 11, 116]
N-mustard derivatives			
$-CH_2-CH_2-I$	RebM	S	[118]

Table B.1.: Overview over the contructs produced for the present thesis. Each step during the production of the construct is given in the workflow steps column. Primers (italic font) or restriction sites used during each step are displayed in parenthesis.

construct name	description	entry constructs	destination	workflow steps (primers/cloning sites)
pBEW101				
pBEW102	lsrA promoter			
pBEW103	pBEW102 with BamHI cloning site	pBEW102		
pBEW104	$rhaP_{BAD}$ promoter	pBEW4b	pBEW103	amplification (*pRha1.fw/rv*), cloning (BglII, BamHI)
pBEW106	pICH413038-somt	pET28MC-somt	pICH413038	amplification (*somt1/2/3/4*), golden gate cloning (BpiI)
pBEW107		pICH51266, pBEW106, pICH41421	pICH75044	golden gate cloning (BsaI)
pBEW1a				
pBEW1b				
pBEW2a				
pBEW2b				
pBEW3a				
pBEW3b				
pBEW4a				
pBEW4b				
pET28-pfomt	*pfomt* gene in pET-28a(+), endogenous NdeI site removed	pQE30-pfomt	pET-28a(+)	mutagenesis (*pfomt1.fw/rv*), amplification (*pfomt2.fw/rv*), cloning (NdeI, EcoRI)
pET20-somt	N-terminal pelB-tag fusion for periplasmic expression		pET20-b(+)	
pET28-somt			pET28-a(+)	
pET28MC-somt				
pET32-somt	N-terminal TrX-tag fusion		pET-32a(+)	
pET41-somt	N-terminal GST-tag fusion		pET-41a(+)	
pUC19*	added BglII site	pUC19	-	mutagenesis (*pUC1.fw/rv*)
pUCB1	pUC19 derivative with lsrA promoter	lsr-XX-DAS	pUC19*	cloning (NdeI, BglII)
pUCB1-sfGFP-DAS+4				

C Affidavit

I hereby declare that this document has been written only by the undersigned and without any assistance from third parties. Furthermore, I confirm that no sources have been used in the preparation of this document other than those indicated in the thesis itself.

Date: . . . . . , Location: . . . . . , Signature: . . . . . .

Bibliography

[1] Paul D. Adams et al. “PHENIX: A comprehensive Python-based system for macromolecular structure solution”. en. In: *Acta Crystallogr. Sect. D Biol. Crystallogr.* 66.2 (Feb. 2010), pp. 213–221.

[2] Agilent Technologies. *QuikChange II Site-Directed Mutagenesis Kit: Instruction Manual.* 2011.

[3] Neda Akbari et al. “Efficient refolding of recombinant lipase from Escherichia coli inclusion bodies by response surface methodology.” In: *Protein Expr. Purif.* 70.2 (Apr. 2010), pp. 254–9.

[4] Martin Alexander and B. K. Lustigman. “Effect of Chemical Structure on Microbial Degradation of Substituted Benzenes”. In: *J. Agric. Food Chem.* 14.4 (July 1966), pp. 410–413.

[5] Oyvind M. Andersen and Kenneth R. Markham, eds. *Flavonoids: Chemistry, Biochemistry and Applications.* 1st ed. Boca Raton (FL): Taylor & Francis Group, 2006.

[6] Bernd Anselment et al. “Experimental optimization of protein refolding with a genetic algorithm”. In: *Protein Sci.* 19.11 (2010), pp. 2085–2095.

[7] Frederick M Ausubel et al. “Current Protocols in Molecular Biology”. In: (2008), p. 23.

[8] Isabelle Benoit et al. “Expression in Escherichia coli, refolding and crystallization of Aspergillus niger feruloyl esterase A using a serial factorial approach.” In: *Protein Expr. Purif.* 55.1 (Sept. 2007), pp. 166–74.

[9] Olivier Binda et al. “A Chemical Method for Labeling Lysine Methyltransferase Substrates”. In: *ChemBioChem* 12.2 (2011), pp. 330–334.

[10] Ian R Bothwell and Minkui Luo. “Large-scale, protection-free synthesis of Se-adenosyl-l-selenomethionine analogues and their application as cofactor surrogates of methyltransferases”. In: *Org. Lett.* 16.11 (2014), pp. 3056–3059.

[11] Ian R. Bothwell et al. “Se-adenosyl-L-selenomethionine cofactor analogue as a reporter of protein methylation”. In: *J. Am. Chem. Soc.* 134.36 (2012), pp. 14905–14912.

[12] George E. P. Box, J. Stuart Hunter, and William G. Hunter. *Statistics for Experimenters: Design, Innovation, and Discovery*. 2nd ed. New York: Wiley-Interscience, 2005.

[13] Jhong-Min Chen et al. “Structural Insight into MtmC, a Bifunctional Ketoreductase-Methyltransferase Involved in the Assembly of the Mithramycin Trisaccharide Chain”. In: *Biochemistry* 54.15 (2015), pp. 2481–2489.

[14] Jih Jung Chen et al. “Dihydroagarofuranoid sesquiterpenes, a lignan derivative, a benzenoid, and antitubercular constituents from the stem of Microtropis japonica”. In: *J. Nat. Prod.* 71.6 (2008), pp. 1016–1021.

[15] Vincent B Chen et al. “MolProbity: all-atom structure validation for macromolecular crystallography.” In: *Acta Crystallogr. D. Biol. Crystallogr.* 66.Pt 1 (Jan. 2010), pp. 12–21.

[16] Al Claiborne and Irwin Fridovich. “Chemical and Enzymatic Intermediates in the Peroxidation of o-Dianisidine by Horseradish Peroxidase. 1. Spectral Properties of the Products of Dianisidine Oxidation”. In: *Biochemistry* 18 (1979), pp. 2324–2329.

[17] Yuntao Dai et al. “Natural deep eutectic solvents as new potential media for green technology.” In: *Anal. Chim. Acta* 766 (Mar. 2013), pp. 61–8.

[18] Christian Dalhoff et al. “Direct transfer of extended groups from synthetic cofactors by DNA methyltransferases.” In: *Nat. Chem. Biol.* 2.1 (2006), pp. 31–32.

[19] Christian Dalhoff et al. “Synthesis of S-adenosyl-L-methionine analogs and their use for sequence-specific transalkylation of DNA by methyltransferases.” In: *Nat. Protoc.* 1.4 (2006), pp. 1879–1886.

[20] Martin Dippe, Lars Dressler, and Renate Ulbrich-Hofmann. “Fe(III)-resorcylate as a spectrophotometric probe for phospholipid-cation interactions.” In: *Anal. Biochem.* 445 (Jan. 2014), pp. 54–9.

[21] Martin Dippe et al. “Engineering of a Mg2+-dependent O-methyltransferase towards novel regiospecificity”. In: *Manuscr. Submitt.* (2015).

[22] Martin Dippe et al. “Rationally engineered variants of S-adenosylmethionine (SAM) synthase: reduced product inhibition and synthesis of artificial cofactor homologues.” en. In: *Chem. Commun. (Camb).* 51.17 (Feb. 2015), pp. 3637–40.

[23] Toru Egawa, Akiyo Kameyama, and Hiroshi Takeguchi. “Structural determination of vanillin, isovanillin and ethylvanillin by means of gas electron diffraction and theoretical calculations”. In: *J. Mol. Struct.* 794 (2006), pp. 92–102.

[24] Elsevier. *Reaxys, version 2.19790.2*.

[25] P. Emsley et al. “Features and development of Coot”. In: *Acta Crystallogr. Sect. D Biol. Crystallogr.* 66.4 (2010), pp. 486–501.

[26] Carola Engler, Romy Kandzia, and Sylvestre Marillonnet. “A one pot, one step, precision cloning method with high throughput capability”. In: *PLoS One* 3.11 (Jan. 2008), e3647.

[27] Philip Evans. “Scaling and assessment of data quality”. In: *Acta Crystallogr. Sect. D Biol. Crystallogr.* 62.1 (Jan. 2006), pp. 72–82. arXiv: *S0907444905036693* [doi:10.1107].

[28] Matthew W Freyer and Edwin a Lewis. “Isothermal titration calorimetry: experimental design, data analysis, and probing macromolecule/ligand binding and kinetic interactions.” In: *Methods Cell Biol.* 84.07 (Jan. 2008), pp. 79–113.

[29] Eva K Freyhult, Karl Andersson, and Mats G Gustafsson. “Structural modeling extends QSAR analysis of antibody-lysozyme interactions to 3D-QSAR.” In: *Biophys. J.* 84.4 (Apr. 2003), pp. 2264–72.

[30] Steffen Friedrich and Frank Hahn. “Opportunities for enzyme catalysis in natural product chemistry”. In: *Tetrahedron* 71.10 (2015), pp. 1473–1508.

[31] Rafael García-Meseguer et al. “Linking Electrostatic Effects and Protein Motions in Enzymatic Catalysis. A Theoretical Analysis of Catechol O -Methyltransferase”. In: *J. Phys. Chem. B* 119.3 (2015), pp. 873–882.

[32] E. Gasteiger et al. “Protein Identification and Analysis Tools on the ExPASy Server”. In: *Proteomics Protoc. Handb.* Ed. by John M. Walker. Humana Press, 2005, pp. 571–607.

[33] S C Gill and P H von Hippel. “Calculation of protein extinction coefficients from amino acid sequence data.” In: *Anal. Biochem.* 182.2 (Nov. 1989), pp. 319–26.

[34] Markus Grammel and Howard C Hang. “Chemical reporters for biological discovery.” In: *Nat. Chem. Biol.* 9.8 (2013), pp. 475–84.

[35] Erich Grotewold, ed. *The Science of Flavonoids*. 1st ed. New York: Springer, 2006.

[36] Han Guo et al. “Profiling substrates of protein arginine N-methyltransferase 3 with S-adenosyl-L-methionine analogues”. In: *ACS Chem. Biol.* 9.2 (2014), pp. 476–484.

[37] Albert Hofmann. *Die Mutterkornalkaloide*. Solothurn: Nachtschatten Verlag, 2000.

[38] Scott Horowitz et al. “Conservation and functional importance of carbon-oxygen hydrogen bonding in AdoMet-dependent methyltransferases”. In: *J. Am. Chem. Soc.* 135.41 (2013), pp. 15536–15548.

[39] Ze Lin Huang et al. “Deep eutectic solvents can be viable enzyme activators and stabilizers”. In: *J. Chem. Technol. Biotechnol.* October 2013 (2014).

[40] Ruth Huey et al. “A semiempirical free energy force field with charge-based desolvation.” In: *J. Comput. Chem.* 28.6 (Apr. 2007), pp. 1145–52.

[41] Mwafaq Ibdah et al. “A Novel Mg2+-dependent O-Methyltransferase in the Phenylpropanoid Metabolism of Mesembryanthemum crystallinum”. In: *J. Biol. Chem.* 278.45 (Nov. 2003), pp. 43961–43972.

[42] I Chemical Identity. “Chemical summary for vanillin”. In: *Evaluation* 121 (1996), pp. 1–8.

[43] Kabirul Islam et al. “Expanding cofactor repertoire of protein lysine methyltransferase for substrate labeling”. In: *ACS Chem. Biol.* 6.7 (2011), pp. 679–684.

[44] PD Josephy, T Eling, and RP Mason. “The horseradish peroxidase-catalyzed oxidation of 3, 5, 3’, 5’-tetramethylbenzidine. Free radical and charge-transfer complex intermediates.” In: *J. Biol. Chem.* 257 (1982), pp. 3669–3675.

[45] Wolfgang Kabsch. “Automatic processing of rotation diffraction data from crystals of initially unknown symmetry land cell constants”. In: *J. Appl. Crystallogr.* 26.pt 6 (Dec. 1993), pp. 795–800.

[46] Wolfgang Kabsch. “Integration, scaling, space-group assignment and post-refinement”. In: *Acta Crystallogr. Sect. D Biol. Crystallogr.* 66.2 (Feb. 2010), pp. 133–144.

[47] Wolfgang Kabsch. “Xds”. In: *Acta Crystallogr. Sect. D Biol. Crystallogr.* 66.2 (Feb. 2010), pp. 125–132.

[48] K Kajiya et al. “Molecular bases of odor discrimination: Reconstitution of olfactory receptors that recognize overlapping sets of odorants.” In: *J. Neurosci.* 21.16 (2001), pp. 6018–6025.

[49] Selin Kara et al. “Recent trends and novel concepts in cofactor-dependent biotransformations”. In: *Appl. Microbiol. Biotechnol.* 98.4 (2014), pp. 1517–1529.

[50] Adler Kirk. “No Title”. In: *Acta Chem. Scand.* 24 (1970), pp. 3379–3388.

[51] Youichi Kondou et al. “cDNA Libraries”. In: *Methods Mol. Biol.* 729 (2011), pp. 183–197.

[52] Jakub G. Kopycki et al. “Biochemical and Structural Analysis of Substrate Promiscuity in Plant Mg2+-Dependent O-Methyltransferases”. In: *J. Mol. Biol.* 378.1 (Apr. 2008), pp. 154–164.

[53] Gerhard Krammer and Jenny Hartmann-Schreier. *Römpp Enzyklopädie Online*. 2015.

[54] Ulrich K Laemmli. “Cleavage of structural proteins during the assembly of the head of bacteriophage T4.” In: *Nature* 227.5259 (1970), pp. 680–685.

[55] Brian J. C. Law et al. “Site-specific bioalkylation of rapamycin by the RapM 16-O-methyltransferase”. In: *Chem. Sci.* (2015), pp. 2885–2892.

[56] Bobby W K Lee et al. “Enzyme-catalyzed transfer of a ketone group from an S-adenosylmethionine analogue: A tool for the functional analysis of methyltransferases”. In: *J. Am. Chem. Soc.* 132.11 (2010), pp. 3642–3643.

[57] Jakob P. Ley et al. “Evaluation of bitter masking flavanones from Herba Santa (Eriodictyon californicum (H. & A.) Torr., Hydrophyllaceae)”. In: *J. Agric. Food Chem.* 53.15 (2005), pp. 6061–6066.

[58] Jiaojie Li, Hua Wei, and Ming Ming Zhou. “Structure-guided design of a methyl donor cofactor that controls a viral histone H3 lysine 27 methyltransferase activity”. In: *J. Med. Chem.* 54.21 (2011), pp. 7734–7738.

[59] Christopher A Lipinski. “Lead- and drug-like compounds: the rule-of-five revolution.” In: *Drug Discov. Today. Technol.* 1.4 (Dec. 2004), pp. 337–41.

[60] Christopher A Lipinski et al. “Experimental and computational approaches to estimate solubility and permeability in drug discovery and development settings1PII of original article: S0169-409X(96)00423-1. The article was originally published in Advanced Drug Delivery Reviews 23 (1997) 3”. In: *Adv. Drug Deliv. Rev.* 46.1-3 (Mar. 2001), pp. 3–26.

[61] David K Liscombe, Gordon V Louie, and Joseph P Noel. “Architectures, mechanisms and molecular evolution of natural product methyltransferases.” In: *Nat. Prod. Rep.* 29.10 (Oct. 2012), pp. 1238–50.

[62] Gražvydas Lukinavičius et al. “Enhanced chemical stability of AdoMet analogues for improved methyltransferase-directed labeling of DNA”. In: *ACS Chem. Biol.* 8.6 (2013), pp. 1134–1139.

[63] Minkui Luo. “Current chemical biology approaches to interrogate protein methyltransferases”. In: *ACS Chem. Biol.* 7.3 (2012), pp. 443–463.

[64] Tom J. Mabry, K. R. Markham, and M. B. Thomas. *The Systematic Identification of Flavonoids*. Berlin, Heidelberg: Springer Berlin Heidelberg, 1970.

[65] Van Mai and Lindsay R Comstock. “Synthesis of an azide-bearing N-mustard analogue of S-adenosyl-L-methionine”. In: *J. Org. Chem.* 76.24 (2011), pp. 10319–10324.

[66] Savvas C Makrides and Savvas C Makrides. “Strategies for Achieving High-Level Expression of Genes in Escherichia coli”. In: *Microbiol. Rev.* 60.3 (1996), pp. 512–538.

[67] S. V. Mani, D. W. Connell, and R. D. Braddock. “Structure activity relationships for the prediction of biodegradability of environmental pollutants”. en. In: *Crit. Rev. Environ. Control* 21.3-4 (Jan. 1991), pp. 217–236.

[68] Kavitha Marapakala et al. “A disulfide-bond cascade mechanism for arsenic(III) S -adenosylmethionine methyltransferase”. In: *Acta Crystallogr. Sect. D Biol. Crystallogr.* 71.3 (2015), pp. 505–515.

[69] E. Neil G Marsh, Dustin P. Patterson, and Lei Li. “Adenosyl radical: Reagent and catalyst in enzyme reactions”. In: *ChemBioChem* 11.5 (2010), pp. 604–621.

[70] Airlie J. McCoy. “Solving structures of protein complexes by molecular replacement with Phaser”. In: *Acta Crystallogr. Sect. D Biol. Crystallogr.* 63.1 (Jan. 2006), pp. 32–41.

[71] Airlie J. McCoy et al. “Phaser crystallographic software”. In: *J. Appl. Crystallogr.* 40.4 (Aug. 2007), pp. 658–674.

[72] Edoardo Mentasti and Ezio Pelizzetti. “Reactions between iron(III) and catechol (o-dihydroxybenzene). part I. Equilibria and kinetics of complex formation in aqueous acid solution”. en. In: *J. Chem. Soc. Dalt. Trans.* 23 (Jan. 1973), p. 2605.

[73] Garrett M Morris et al. “AutoDock4 and AutoDockTools4: Automated docking with selective receptor flexibility.” In: *J. Comput. Chem.* 30.16 (Dec. 2009), pp. 2785–91.

[74] Yuri Motorin et al. “Expanding the chemical scope of RNA:methyltransferases to site-specific alkynylation of RNA for click labeling”. In: *Nucleic Acids Res.* 39.5 (2011), pp. 1943–1952.

[75] Garib N. Murshudov, Alexei a. Vagin, and Eleanor J. Dodson. “Refinement of macromolecular structures by the maximum-likelihood method”. In: *Acta Crystallogr. Sect. D Biol. Crystallogr.* 53.3 (May 1997), pp. 240–255.

[76] Janet Newman. “Novel buffer systems for macromolecular crystallization”. In: *Acta Crystallogr. Sect. D Biol. Crystallogr.* 60.3 (2004), pp. 610–612.

[77] Siwen Niu et al. “Characterization of a sugar-O-methyltransferase TiaS5 affords new Tiacumicin analogues with improved antibacterial properties and reveals substrate promiscuity.” In: *Chembiochem* 12.11 (July 2011), pp. 1740–8.

[78] Novagen. *pET System Manual.* 11th ed. Darmstadt: EMD Chemicals, 2010.

[79] Tanesha Osborne et al. “In situ generation of a bisubstrate analogue for protein arginine methyltransferase 1.” In: *J. Am. Chem. Soc.* 130.14 (2008), pp. 4574–4575.

[80] Ira Palmer and Paul T. Wingfield. “Preparation and extraction of insoluble (Inclusion-body) proteins from Escherichia coli”. In: *Curr. Protoc. Protein Sci.* 1.SUPPL.70 (Nov. 2012), Unit6.3.

[81] Wibke Peters et al. “Enzymatic site-specific functionalization of protein methyltransferase substrates with alkynes for click labeling”. In: *Angew. Chemie - Int. Ed.* 49.30 (2010), pp. 5170–5173.

[82] Harold R. Powell. “The Rossmann Fourier autoindexing algorithm in MOSFLM”. In: *Acta Crystallogr. Sect. D Biol. Crystallogr.* 55.10 (1999), pp. 1690–1695.

[83] R Core Team. *R: A Language and Environment for Statistical Computing*. R Foundation for Statistical Computing. Vienna, Austria, 2015.

[84] Randy J. Read. “Pushing the boundaries of molecular replacement with maximum likelihood.” en. In: *Acta Crystallogr. Sect. D Biol. Crystallogr.* 57.Pt 10 (Jan. 2001), pp. 1373–1382.

[85] Michael Richter. “Functional diversity of organic molecule enzyme cofactors.” In: *Nat. Prod. Rep.* 30.10 (2013), pp. 1324–45.

[86] M. G. Rossmann and D. M. Blow. “The detection of sub-units within the crystallographic asymmetric unit”. In: *Acta Crystallogr.* 15.1 (Jan. 1962), pp. 24–31.

[87] Michael G. Rossmann. “Molecular replacement - Historical background”. In: *Acta Crystallogr. - Sect. D Biol. Crystallogr.* 57.10 (Sept. 2001), pp. 1360–1366.

[88] Rainer Rudolph and Hauke Lilie. “In vitro folding of inlusion body proteins”. In: *FASEB J.* 10 (1996), pp. 49–56.

[89] Bernhard Rupp. *Biomolecular Crystallography: Principles, Practice, and Application to Structural Biology*. 1st ed. New York: Garland Science, 2009, p. 800.

[90] J H Ruth. “Odor thresholds and irritation levels of several chemical substances: a review.” In: *Am. Ind. Hyg. Assoc. J.* 47.3 (1986), A142–A151.

[91] J Sambrook and D W Russell. *Molecular Cloning: A Laboratory Manual*. 3rd ed. Cold Spring Harbor (NY, USA): Cold Spring Harbor Laboratory Press, 2001.

[92] Cleydson Breno R Santos et al. “A SAR and QSAR study of new artemisinin compounds with antimalarial activity”. In: *Molecules* 19.1 (2014), pp. 367–399.

[93] Daniela Schulz, Josephin Marie Holstein, and Andrea Rentmeister. “A chemo-enzymatic approach for site-specific modification of the RNA cap”. In: *Angew. Chemie - Int. Ed.* 52.30 (2013), pp. 7874–7878.

[94] Daniela Schulz and Andrea Rentmeister. “Current Approaches for RNA Labeling in Vitro and in Cells Based on Click Reactions”. In: *ChemBioChem* 15.16 (2014), pp. 2342–2347.

[95] N. Schweigert, a. J B Zehnder, and R. I L Eggen. “Chemical properties of catechols and their molecular modes of toxic action in cells, from microorganisms to mammals”. In: *Environ. Microbiol.* 3.2 (2001), pp. 81–91.

[96] Stanley K. Shapiro and Dimis J. Ehninger. “Methods for the analysis and preparation of adenosylmethionine and adenosylhomocysteine”. In: *Anal. Biochem.* 15.2 (May 1966), pp. 323–333.

[97] Alexander Shulgin and Ann Shulgin. *TiHKAL - The Continuation*. Ed. by Dan Joy. 1st ed. Berkeley: Transform Press, 1997.

[98] Sigma-Aldrich. *Technical Bulletin no. 2003-03: freezing of microbial samples prior to testing. Parenteral Drug Association.* 2003.

[99] Shanteri Singh et al. “Facile chemoenzymatic strategies for the synthesis and utilization of S-adenosyl-L-methionine analogues”. In: *Angew. Chemie - Int. Ed.* 53.15 (2014), pp. 3965–3969.

[100] Harald Stecher et al. “Biocatalytic Friedel-Crafts alkylation using non-natural cofactors.” In: *Angew. Chem. Int. Ed. Engl.* 48.50 (Jan. 2009), pp. 9546–8.

[101] L. S. Stepanenko et al. “Characteristics of the far-eastern lichen Cetraria islandica”. In: *Chemsitry Nat. Prod.* 32.1 (1996), pp. 66–70.

[102] Anna-Winona Struck et al. “S-Adenosyl-Methionine-Dependent Methyltransferases: Highly Versatile Enzymes in Biocatalysis, Biosynthesis and Other Biotechnological Applications.” In: *Chembiochem* (Nov. 2012), pp. 1–15.

[103] F William Studier. “Protein production by auto-induction in high density shaking cultures.” In: *Protein Expr. Purif.* 41.1 (May 2005), pp. 207–234. arXiv: *NIHMS150003*.

[104] Martin Tengg et al. “Molecular characterization of the C-methyltransferase NovO of Streptomyces spheroides, a valuable enzyme for performing Friedel–Crafts alkylation”. In: *J. Mol. Catal. B Enzym.* 84 (Dec. 2012), pp. 2–8.

[105] Marie Thomsen et al. “Chemoenzymatic synthesis and in situ application of S-adenosyl-L-methionine analogs.” In: *Org. Biomol. Chem.* 11.43 (2013), pp. 7606–10.

[106] Oleg Trott and Arthur J Olson. “AutoDock Vina: improving the speed and accuracy of docking with a new scoring function, efficient optimization, and multithreading.” In: *J. Comput. Chem.* 31.2 (Jan. 2010), pp. 455–61.

[107] Alexei a. Vagin et al. “REFMAC5 dictionary: Organization of prior chemical knowledge and guidelines for its use”. en. In: *Acta Crystallogr. Sect. D Biol. Crystallogr.* 60.12 I (Nov. 2004), pp. 2184–2195.

[108] Thomas Vogt. “Regiospecificity and kinetic properties of a plant natural product O-methyltransferase are determined by its N-terminal domain”. In: *FEBS Lett.* 561.1-3 (Mar. 2004), pp. 159–162.

[109] Rui Wang and Minkui Luo. “A journey toward bioorthogonal profiling of protein methylation inside living cells”. In: *Curr. Opin. Chem. Biol.* 17.5 (2013), pp. 729–737.

[110] Rui Wang, Weihong Zheng, and Minkui Luo. “A sensitive mass spectrum assay to characterize engineered methionine adenosyltransferases with S-alkyl methionine analogues as substrates”. In: *Anal. Biochem.* 450.1 (2014), pp. 11–19.

[111] Rui Wang et al. “Formulating a fluorogenic assay to evaluate S-adenosyl-L-methionine analogues as protein methyltransferase cofactors”. In: *Mol. Biosyst.* 7.11 (2011), p. 2970.

[112] Rui Wang et al. “Labeling substrates of protein arginine methyltransferase with engineered enzymes and matched S-adenosyl-l-methionine analogues”. In: *J. Am. Chem. Soc.* 133.20 (2011), pp. 7648–7651.

[113] Melissa Swope Willis et al. “Investigation of protein refolding using a fractional factorial screen: a study of reagent effects and interactions.” In: *Protein Sci.* 14.7 (2005), pp. 1818–1826.

[114] Sophie Willnow et al. “A Selenium-Based Click AdoMet Analogue for Versatile Substrate Labeling with Wild-Type Protein Methyltransferases”. In: *ChemBioChem* 13.8 (2012), pp. 1167–1173.

[115] Martyn D. Winn et al. “Overview of the CCP4 suite and current developments”. In: *Acta Crystallogr. Sect. D Biol. Crystallogr.* 67.4 (Apr. 2011), pp. 235–242.

[116] Jaclyn M. Winter et al. “Expanding the structural diversity of polyketides by exploring the cofactor tolerance of an inline methyltransferase domain”. In: *Org. Lett.* 15.14 (2013), pp. 3774–3777.

[117] Yingying Wu et al. “N-Methylation of the Amide Bond by Methyltransferase Asm10 in Ansamitocin Biosynthesis”. In: *ChemBioChem* 12.11 (2011), pp. 1759–1766.

[118] Changsheng Zhang et al. “Natural product diversification using a non-natural cofactor analogue of S-adenosyl-L-methionine”. In: *J. Am. Chem. Soc.* 128.9 (2006), pp. 2760–2761.

[119] Jun Zhang et al. “Arsenic Methylation and Volatilization by Arsenite S -Adenosylmethionine Methyltransferase in Pseudomonas alcaligenes NBRC14159”. In: *Appl. Environ. Microbiol.* 81.8 (2015), pp. 2852–2860.

Acronyms

Å Ångström, 0.1 nm

ABPP activity based protein profiling 33
AC-9 anthracene-9-carboxylic acid 20
ATP adenosine triphosphate 20

BisTris 2-[Bis(2-hydroxyethyl)amino]-2-(hydroxymethyl)propane-1,3-diol
B-PER bacterial protein extraction reagent

CCP4 Collaborative Computational Project No. 4 22, 23
CD circulary dichroism 10
***C*-MT** *C*-methyl transferase 32
COMT catechol O-methyl transferase 13
Coot Crystallographic Object-Oriented Toolkit 23
CV column volumes

DMSO dimethyl sulfoxide 21, 36
DNA desoxyribonucleic acid
DNA MT DNA methyl transferase vi, 30, 31
DoE design of experiments 18
DTT dithiothreitol; (2*S*,3*S*)-1,4-bis(sulfanyl)butane-2,3-diol

EDTA ethylenediaminetetraacetic acid 15, 17, 18, 26

FFD fractional factorial design viii, 18, 19
FPLC fast protein liquid chromatography 17, 28
FT Fourier transformation 22

GdmCl guanidinium hydrochloride
GFP green fluorescent protein 23
GOD glucose oxidase 24, 63
GSH glutathione, γ-L-glutamyl-L-cysteinylglycine 18, 24, 26

GSSG glutathione disulfide 18

HEPES 2-[4-(2-hydroxyethyl)piperazin-1-yl]ethanesulfonic acid
HIC hydrophobic interaction chromatography 28
HPLC high-performance liquid chromatography 13, 20, 26, 29
HRP horseradish peroxidase 24

IB inclusion body 17, 19
IEX ion exchange chromatography 20
IMAC immobilized metal affinity chromatography
IPB Leibniz-Institute of Plant Biochemistry
IPTG isopropyl-D-thiogalactopyranosid 14, 16, 17
ITC Isothermal Titration Calorimetry 28, 33, 63

LB lysogeny broth 12, 13, 16
LC/MS liquid chromatography coupled mass-spectrometry 34

MES 2-(*N*-morpholino)ethanesulfonic acid
MLU Martin-Luther-Universität
MMT L-malic acid/MES/Tris 6, 28
MR molecular replacement
MT methyl transferase vi, viii, 30–33, 46
MTP micro-titer plate 21–24, 63
MW molecular weight 15
MWCO molecular weight cut-off

NADES natural deep eutectic solvent viii, 7, 21, 61
NPS nitrogen, phosphate, sulfate buffer
NRPS non-ribosomal peptide synthase 30
NTA nitrilo triacetic acid 17

***O*-MT** *O*-methyl transferase 24, 26, 29, 32

PAGE polyacrylamide gel electrophoresis 14, 15, 19, 20, 28
PBS phosphate buffered saline 14, 19, 23
PCH propane-1,2-diol/choline chloride,NADES-mixture 21
PCR polymerase chain reaction 10, 11
PDA photo diode array 29
PDB Protein Data Base 22, 23
PFOMT phenylpropanoid and flavonoid O-methyl transferase vii, 13, 16, 21–24, 28, 33–37, 63
PHENIX Phyton-based Hierarchial Environment for Integrated Xtallography 23

PKS poly ketide synthase 30
PMSF phenylmethylsulfonylfluoride
P-MT protein methyl transferase vi, 30–32

QSAR quantitative structure activity relationship 30

rmsd root mean squared deviation 38
rna ribonucleic acid vi, 31
RT room temperature

SAE *S*-adenosyl-L-ethionine, (2*S*)-2-amino-4-[[(2*S*,3*S*,4*R*,5*R*)-5-(6-aminopurin-9-yl)-3,4-dihydroxyoxolan-2-yl]methyl-ethylsulfonio]butanoat 20, 21, 31, 33, 34, 36
SAH *S*-adenosyl-L-homocysteine 18, 26, 33, 36, 37
SAM *S*-adenosyl-L-methionine vi–viii, 20, 24, 26, 30–35, 41, 46
SAMS *S*-adenosylmethionine synthase 20
SAR structure activity relationship 30
SDS sodium dodecylsulfate 7, 14, 15, 19, 20, 28
***Se*AM** *Se*-adenosyl selenomethionine vi, 31, 32, 46
SOMT-2 soy O-methyl transferase 13, 16–20, 28
SSG succinate/sodium phosphate/glycine 7

TB terrific broth 13
TCA trichloro acetic acid 14, 15, 19, 26, 28
Ti-plasmid tumor inducing plasmid 8, 63
Tris tris(hydroxymethyl)-aminomethane

U enzyme unit; measure for enzymatic activity (1 U = 1 µmole/min = 1/60 µkat)
UV/VIS ultra violet/visible (light spectrum) 20, 29

V volume

ZYP N-*Z*-amine, *y*east extract, *p*hosphate 16, 63

Glossary

GOD Glucose oxidase is an enzyme.... 60

Isothermal Titration Calorimetry (ITC) Fill in description here 61

MTP Micro-titer plate. Small format rectangular plastic plate containing wells to allow for storage of multiple small samples or the containment multiple simultaneous reactions. Typical sizes include 24, 96 and 384-wells 61

PFOMT Phenylpropanoid and flavonoid O-methyl transferase from *Mesembryanthemum crystallinum*, which was first described by Ibdah et al. in 2003 [41] 61

Ti-plasmid Commonly found plasmids in *A. tumefaciens* and *A. rhizogenes* that confer virulence 62

ZYP-5052 Autoinduction medium developed by Studier [103]. The naming stems from the components N-*Z*-amine, *y*east extract and *p*hosphate. The numbering designates the composition; e.g. 5052 refers to 0.5 % glycerol, 0.05 % glucose and 0.2 % lactose. 62